Available online at www.sciencedirect.com
SCIENCE DIRECT®
Journal of volcanology and geothermal research
ELSEVIER
Journal of Volcanology and Geothermal Research 122 (2003) 7–50
www.elsevier.com/locate/jvolgeores

The mechanism of volcanic eruptions (a steady state approach)

Yu.B. Slezin

Institute of Volcanic Geology and Geochemistry FED RAS, Piip Blvd. 9, 683006 Petropavlovsk-Kamchatsky, Russia

Received 13 December 2001; accepted 17 September 2002

Abstract

A theory of a volcanic eruption as a steady magma flow from a magma chamber to the surface is described. Magma is considered as a two-component two-phase medium and magma flow is steady, one-dimensional and isothermal. Mass and momentum exchange between condensed and gaseous phases is assumed to be in equilibrium with nucleation of bubbles as a fast process at small oversaturations. Three basic flow structures in a conduit are recognized and three resulting types of eruption are described. (1) In the discrete gas separation (DGS) flow, melt with discrete gas bubbles erupts. This type includes lava eruptions and Strombolian activity. (2) In the dispersion regime there is continuous eruption of a gas-pyroclastic suspension. Catastrophic explosive eruptions are included in this type. (3) Here a partly destroyed foam is erupted with permeable structure that allows gas escape. Near the surface this structure evolves with an increase in permeability and a decrease in the total porosity. This type corresponds to lava dome extrusions. A criterion dividing DGS flow from the other two regimes is obtained: $Di = U\eta n^{1/3} a/c_0$, where U is the magma ascent velocity, η is magma viscosity, n is number of bubble nuclei in a unit mass of magma, a is the solubility coefficient for volatiles in magma and c_0 is the volatile content. The boundary between the dispersion regime and the partly destroyed foam regime depends on U, c_0 and particle size d_p. For the dispersion regime the basic governing parameters are: magma chamber depth H, conduit conductivity $\sigma = b^2/\eta$ (b is the characteristic cross-dimension of the conduit), and excess pressure in the magma chamber. Instability of the dispersion regime is investigated numerically. The dependence of magma discharge rate on the governing parameters is described as a combination of equilibrium surfaces with cusp catastrophes. Magma chamber depth is a 'splitting' parameter in most cusps and controls the existence of unstable magma flow with sharp regime changes. Catastrophic rise of eruption intensity is possible if $H < H_{cr}$. The critical chamber depth H_{cr} depends approximately linearly on c_0 and is about 15 km at $c_0 = 0.05$. Some scenarios of eruption evolution are described in a steady state approximation, and the mechanism of catastrophic explosive eruptions is proposed. The theory is applied to well documented eruptions (Tolbachik, 1975–1976, and Mount St. Helens, 1980). The theory can also describe changes in a volcanic system, such as destruction of the conduit or chamber walls, destruction of the edifice, changes in magma composition, and caldera subsidence due to magma evacuation.

Keywords: volcanic eruption; steady state; two-phase flow regime; critical conditions

0377-0273/02/$ – see front matter © 2002 Elsevier Science B.V. All rights reserved.
PII: S0377-0273(02)00464-X

1. Introduction

Volcanism is a global phenomenon and study of it includes many aspects and approaches. In this paper the physical mechanism of eruption is discussed. I have used only a steady state approach, which cannot describe all the details and complexities of volcanic processes. However, this approach is an important starting point as it helps to describe and to understand the general features of eruptions, including abrupt transitions from one steady regime to another. The objective of this extensive paper is to review and summarize a large body of research results on the theory of volcanic eruptions developed by the author over the last two decades. Principally it concerns the nature of eruption instability and abrupt changes in eruptive style. This work has largely been published in Russian and is not well known within the international community. Although there are some similarities and parallel developments in the western scientific literature there are fundamental aspects of the research results, concepts and approach which are different. Some of these concepts are emerging outside Russia and so it is timely to publish a synopsis both to familiarize a broader community with interesting results and perhaps to avoid the reinvention of the wheel. I will consider some studies (mostly made after mine), which are partly related to my work. A full comparison cannot be done properly in the limits of this paper, and I apologize to those whose investigations escape this discussion.

1.1. Definitions and formulation of the problem

A *volcanic eruption* is a dynamical process of outflow that is characterized as follows: (1) mechanical properties, composition, and structure of the erupted products; (2) their mass rate of eruption; (3) their velocity; (4) the flow regime, namely the way these characteristics change in time. An eruption is also an *event*, separated from other similar events by a *rest* (or *dormant*) *interval*. Rest is the second of two possible states of an active volcano. *Long-term volcanic activity* is an alternating succession of those two fundamental states. Eruptions can be treated in two respects: as a *process of outflow* and the *evolution of this outflow* over the course of the event.

The direct way to obtain quantitative information about an eruption is by measuring flow characteristics of volcanic eruptions. These measurements are very difficult to obtain, especially in intensive catastrophic eruptions. Most information can only be obtained indirectly, such as by interpretation of measurements made after an eruption, observations at a great distance, and measurements of disturbances and changes in the environment caused by the eruption. Interpretation of such information requires theoretical models. Eruption is the final stage of processes at depth, including origin, formation and transport to the surface of magma; and starts the processes of dispersal of the products. Consequently the study of eruption mechanisms can be divided into two problems: *internal* and *external*. The *external problem* includes the description of the transport of volcanic products from the moment of emerging to the moment of their primary deposition or dissipation in the atmosphere. The *internal problem* concerns describing the dependence of the eruption on the characteristics of the magma system and on external influences. The internal problem involves construction of a *theoretical model* of these processes.

This work concerns the internal problem. Basic regimes of eruption and their evolution, with conditions of their realization, stability limits, and the influence of external factors are investigated using a steady state approach. An approach to predicting hazards of a volcano according to the basic information on the structure and state of its magma system is suggested. Theoretical results are applied to two of the most completely studied eruptions: those of Tolbachik 1975–1976 in Kamchatka, Russia and Mount St. Helens 1980 in Washington State, USA. These eruptions are of quite different types with different magmas and different scenarios. The author took part in the study of the Tolbachik eruption and observations made on this eruption motivated this work.

1.2. A brief review of research

Early studies of volcanic eruptions were con-

cerned with classification. Lacroix (1904), Mercalli (1907) and Jaggar (Luchitsky, 1971) classified the main types of eruption on the basis of the concentration of volatiles in magma and magma viscosity. Escher (1933) and Sonder (Luchitsky, 1971) introduced the magma chamber depth as a control on eruptive type. Early model concepts were only qualitative and largely speculative. The systematic development of the physical concepts of eruption mechanisms began in the middle of the 20th century. Graton (1945) first formulated the physical problem and introduced the term *magma system of a volcano*. Graton recognized that under some conditions in a volcanic conduit a *foam* of close-packed bubbles must form, which must be treated physically as a *new phase*. Verhoogen (1951) consistently described the process of degassing of ascending magma and obtained some quantitative relations.

The contemporary period of theoretical modeling of volcanic eruptions was initially stimulated by planetary research (McGetchin and Ullrich, 1973). A model describing magma flow in a conduit as a steady one-velocity (homogeneous) two-phase flow in a fissure with elastic walls was presented by Wilson et al. (1980). The problem of bubble rise through ascending magma was first investigated by Slezin (1979), who identified different two-velocity flow regimes. Wilson and Head (1981) considered the same problem using different assumptions. Subsequently, numerous studies have developed more elaborate and complicated models. Investigations proceeded in the western countries and in Russia independently and Russian (my) works were not known in the west, leading to duplication of efforts. This paper summarizes some of the author's works on the dynamics of explosive volcanic eruptions published in Russian from 1979 to 1995. These investigations anticipated later research in the west, and also included new concepts. I refer the reader to reviews by Sparks et al. (1997), Papale (1998) and Melnik (2000). I cite only work that is directly complementary or overlapping with mine.

Model developments have included new substantial parameters and new approaches. Some of those new approaches and additional parameters were first considered in my investigations published in Russian. These included two-velocity (non-homogeneous) and quasi-steady problems, multiple solutions for the steady flow, discovery of flow instability and recognition of sharp changes in the eruption intensity and style (Slezin, 1979, 1983, 1984, 1991). These and other related studies were summarized by Slezin (1998). Some later studies in the west partly overlapped with these studies (Wilson and Head, 1981; Jaupart and Allegre, 1991; Dobran, 1992; Woods and Koyaguchi, 1994; Melnik and Sparks, 1999; Melnik, 2000). Only in recent publications (Melnik and Sparks, 1999; Melnik, 2000; Barmin et al., 2002) have preceding Russian results been used.

2. Volcanoes as dynamic systems

2.1. The magma system of a volcano

Volcanism is the result of melt generation in the upper mantle and crust and its transport to the surface. For eruption modeling it is sufficient to assume that magma is generated locally under certain conditions, which depend on the geothermal gradient, thermal properties of the system and geodynamical setting. Magmas are typically generated by partial melting at depths of several tens of kilometers and are differentiated during ascent. Melting and differentiation decrease density typically by 5–15% relative to the original rock (Clark, 1966; Lebedev and Khitarov, 1979). The difference in density between magma and its surroundings causes ascent of magma, its storage and development of excess pressure in magma chambers. In the relatively plastic mantle, asthenosphere melts with relatively low density and low viscosity rise as discrete jets or columns building a periodical structure (e.g. Fedotov, 1976a,b; Ramberg, 1981). Density differences can cause excess pressures at the head of magma column up to 100 MPa. Because of the mechanical properties of most of the lithosphere and especially of the Earth's crust, the most probable way of magma ascent is through fractures propagating in rigid media by the mechanism of *hydrorupture* induced by an excess magma pressure of no more than 20 MPa (e.g. Popov, 1973; Lister, 1990).

The inhomogeneous structure of the crust allows the formation of intracrustal magma chambers, particularly at horizontal strata boundaries and density interfaces. The shallowest of such chambers are here called *peripheral*. Direct evidence for shallow magma chambers is provided by geological and geophysical data (e.g. Luchitsky, 1971; Balesta, 1981; Ryan, 1987). Because of the mechanism of formation, these chambers are initially expected to be horizontally arranged. Relations between the dimensions of magma chambers and volcanic conduits are such that, with respect to magma flow, the first can be treated by analogy to electric circuits as capacitors with negligible resistance, and the second as elements of resistance with very small capacitance.

2.2. Erupting volcano systems

2.2.1. The system geometry and magma properties

Here the upper part of the system consists of the peripheral magma chamber with a conduit connecting it to the surface. The gaseous phase can exsolve and sharp changes in substance properties and in flow structure can take place. The system is strongy non-linear, and alternation of eruptions and dormant periods is characteristic. Average magma discharge rate is approximately constant over a prolonged period of a volcano's life (Kovalev, 1971; Tokarev, 1977; Crisp, 1984). The total energy of an eruption and duration of the cycle, including the eruption and the preceding dormant period, are correlated positively. The correlation becomes much stronger if groups of eruptions (cycles of activity) are concerned instead of the individual eruptions (Kovalev et al., 1971). This suggests that intermittence of volcanic activity is the result of episodic (periodical) discharge of some reservoir (magma chamber), which was steadily refilled from the deeper parts of the magmatic system (Kovalev, 1971; Kovalev and Slezin, 1974).

A volcanic eruption is typically short compared to the duration of dormant periods. Dormant periods are on average 30 times longer than eruption durations for the island arc volcanoes and on average 60 times more for other volcanoes (Simkin and Siebert, 1984). The magma discharge rate during an eruption must surpass the average feeding rate of the magma chamber in similar proportions, and so the latter in most cases can be neglected. So an erupting volcano will be defined as a 'chamber-conduit' system filled with magma with some extra pressure and isolated in all directions except at the upper end of the conduit, which is open to the atmosphere. Relations between the characteristic dimensions of the magma chamber and the volcanic conduit and between characteristic times of the processes of the magma system during eruption permit analysis of an even simpler system, and the study of quasi-steady state scenarios of magma flow through the conduit caused by the constant (slowly changing) pressure difference. There are a limited number of qualitatively different steady states of such a system, which correspond to the different styles and modes of eruption. The main characteristics of an erupting system are as follows.

2.2.1.1. Magma chamber. Its shape is approximated as an ellipsoid or cylinder nearly isometric or flattened in the vertical direction (Fedotov, 1976a,b). Linear dimensions of the horizontal projection are estimated to be from a few kilometers to a few tens of kilometers (Luchitsky, 1971; Farberov, 1979; Balesta, 1981); there is little reliable information about vertical dimensions. Chamber volume can be from a few to thousands of cubic kilometers. The top of the chamber can be situated at depths of a few to a few tens of kilometers (Zubin et al., 1971; Balesta, 1981).

2.2.1.2. Conduit. Although the initial form of a conduit in the lithosphere is a fissure, after some time focusing of flow can change it to a cylinder. At depth this process is slow, but it can be much faster near the surface, where gas exsolves and the velocity and eroding ability of magma increase. Direct observation of the Tolbachik eruption 1975–1976 shows that transformation of the initial fissure to a circular cylinder (near the surface) took only a few days (Fedotov, 1984). In a dormant period a conduit can become partly solidified starting from its upper part; it may become totally closed and eruption through it would not necessarily resume.

The central conduit of a large stratovolcano is a stable, long-lived structure. This is confirmed by the shape of symmetric stratovolcanoes made by innumerable volcanic eruptions, emerging from the same central crater. However, nearly all individual eruptions inside the central crater occur through outlets with dimensions much smaller than the crater floor diameter and are located in different places on this floor. In eroded volcanoes a large number of intersecting dykes of different ages are observed (Luchitsky, 1971; Sheymovich, 1975; Sheymovich and Patoka, 1980). So, even in the case of many successive eruptions through a single crater, the upper part of the conduit for each eruption initially had the form of a newly born fissure.

Factors influencing dyke propagation include internal magma pressure, magma viscosity and tectonic stresses. Two end member models are commonly assumed: (i) an elastic fissure in which internal pressure is equal to external pressure (e.g. Wilson et al., 1980; Wilson and Head, 1981) and (ii) a rigid fissure with behavior only dependent on hydrostatic and magma dynamics (Slezin, 1983; Giberti and Wilson, 1990; Dobran, 1992). For the latter case a constant fissure geometry is commonly assumed. Here the second model was used. The conduit is considered as a fissure at depths where magma flow is taken as a continuous liquid and as a cylinder near the surface where flow consists of a gas–pyroclastic mixture. The model is appropriate for the Great Tolbachik eruption from observations of lava bombs with cores of sedimentary xenoliths (Slobodskoy, 1977) derived from a depth of at least 2 km (Shanzer, 1978) and covered with droplets of magma stuck to them. So the depth of fragmentation had to be no less than 2 km, which would not be so if the fissure were elastic rather than rigid. In the elastic model the hydrostatic pressure in the conduit would be too high to allow magma and wallrock fragmentation at depths of more than a few hundreds of meters. At greater depths the elasticity of fissure walls could play a more significant role.

2.2.1.3. Magma. Magma in the conduit is a two-component, two-phase medium. The components are volatile and non-volatile; the phases are condensed and gaseous. The non-volatile condensed component consists of silicate matter. The volatile component, assumed to be water, can exist both in condensed (i.e. dissolved in the silicate melt) and in gaseous phases. A second volatile component, CO_2, differs from water by having a larger density and being less soluble in the melt (Kadik and Eggler, 1976; Mysen, 1977; Mysen and Virgo, 1980). These properties influence eruption dynamics (through the position of the fragmentation level) in opposite ways. My estimates (Slezin, 1982a) show that the effect of the gas density increase is stronger than the effect of the decrease of solubility. Substitution of water by CO_2 decreases the volume fraction of gas (when mass fraction is constant) and magma discharge rate, and is approximately equivalent to a decrease of the mass fraction of water, a result consistent with findings by Papale and Polacci (1999).

The water content of magmas is typically a few weight percent (up to 6%). However, magma can erupt outside this range. For example, water can be lost by surface degassing prior to eruption and phreatic water can be added to magma. Additional external water was suggested to explain the extremely water-rich basalts erupted by the Northern Cones of the Tolbachik eruption 1975–1976 (Menyaylov et al., 1980; Fedotov, 1984).

The condensed phase is treated as a liquid when it is the continuous component of the flow and as solid matter when it forms pyroclastic particles. Influence of suspended crystals is not considered except for the inability to dissolve volatile components. Density of the condensed phase is approximated as independent of the concentration of the dissolved volatiles. Magma is assumed to be a Newtonian liquid with constant viscosity. In some studies the strong dependence of viscosity on dissolved water concentration is considered (Barmin and Melnik, 1990; Dobran, 1992; Slezin and Melnik, 1994). Dobran (1992) investigated viscosity dependence on bubble concentration. The dependence of viscosity and some other properties of magmas on the composition, pressure, water content and temperature are now well understood (Shaw, 1972; Lebedev and Khitarov,

1979; Epelbaum, 1980; Persikov, 1984; Dingwell et al., 1993).

The solubility of the volatile component (water) in the melt is considered as dependent on pressure p only (Sparks, 1978):

$$c = ap^{1/2} \quad (1)$$

where c is the mass part of volatile component in liquid phase and a is an approximately constant coefficient, with values typically in the interval 0.0032–0.0064 $MPa^{-1/2}$. The lower figure corresponds to mafic magmas and rather large pressures (about 400–600 MPa) whereas the upper figure corresponds to silicic magmas and the pressure interval from 0 to 100–200 MPa. In many studies $a = 0.0041$ $MPa^{-1/2}$ was assumed (Sparks, 1978; Wilson and Head, 1981). Wilson and Head (1981) modified Eq. 1 for basalts with the exponent 0.7.

During decompression due to magma ascent, equilibrium between the volatile component in the melt and in the gaseous phase is assumed. This assumption is usually reasonable for the bubbles in the melt, but invalid in the gas–pyroclast mixture, where speeds are high. But in the latter case volatiles dissolved in the particles are usually low and one of two extreme assumptions provides good approximations: equilibrium or no gas emission at all. For high-viscosity magmas and rapid flow the assumption of equilibrium may not be valid even in the bubble zone, and in this case diffusion delay of gas emission can take place, which is equivalent to a decrease of the volatile content. An attempt to take into account the diffusion delay was made by Slezin and Melnik (1994). Threshold oversaturation needed for heterogeneous bubble nucleation is not large (about 0.1 MPa; Sparks, 1978; Hurwitz and Navon, 1994), so this is neglected. For magma flow dynamics heterogeneous nucleation not only lowers the threshold of new gas phase generation, but also induces generation of very large numbers of bubble nuclei in a unit volume.

2.2.2. *Physical conditions in the system*

The temperatures of erupting magmas are typically 1000–1200°C for basalts and 700–1000°C for silicic magmas. During magma ascent temperature can be influenced by the following processes: (1) heat loss through the conduit walls; (2) exsolution of volatiles; (3) adiabatic expansion; (4) viscous dissipation; (5) crystallization; (6) exothermic reactions. The first and the third processes involve cooling, the second process can have either sign (Kadik et al., 1971), and the last three processes involve heating. These effects can be approximately estimated as follows.

In the rather 'rigid' case of a fissure conduit 10 km long and 2 m wide and magma ascent velocity 0.2 m s^{-1} the temperature decrease due to maximum heat loss through the walls will be several tens of degrees after 24 h and only a few degrees after 1 month of continuous eruption, according to my calculations. For a wider fissure or for the equivalent cylindrical channel the temperature decrease would be less. The thermal effect of water exsolution is negative when pressure is less than 300 MPa (Kadik et al., 1971) and for albite melt composition is about −10°C per 1% H_2O. Above 300 MPa the effect changes sign. Wilson and Head (1981), referring to Burnham and Davis (1974), stated that the effect of water exsolution is positive and is quantitatively no less than +10°C per 1% H_2O. Expansion and acceleration of magma flow transform thermal energy into kinetic energy. Viscous friction transforms kinetic energy into thermal energy. The resulting effect must be negative and proportional to the resulting kinetic energy of eruption products per unit mass of magma. For equal temperatures of gas and pyroclastics and an average velocity at the conduit exit of 100 m s^{-1}, my estimates give a temperature decrease of about 4°C, and 16°C for 200 m s^{-1}. The heat of crystallization of silicate melt varies from 2×10^5 to 4×10^5 J kg^{-1} (Clark, 1966; Dudarev et al., 1972). In an explosive eruption little or no melt can crystallize, but this process can be important in slow extrusions (Sparks et al., 2000). The thermal effect of crystallization is estimated be no more than a few tens of degrees. Exothermic reactions occur on contact with atmospheric oxygen (Macdonald, 1963; Fedotov, 1984), but this effect is negligible for conduit flow. The total change of magma temperature over the conduit length typically is negative and estimated as no more than a few tens of degrees.

These estimates justify the isothermal approximation.

2.2.2.1. Pressure. A magma chamber is fed ultimately from a deeper zone of magma generation due to hydrostatic forces. The density difference between magma and country rocks can provide an upper limit of magma pressure at the head of magma column that exceeds lithostatic pressure by a few hundreds of MPa. However, this limit can never be reached because dykes form and propagate to the surface. Lithostatic pressure for the chambers at different depths (4–30 km) should be from 100 to 700 MPa. An excess pressure of 20 MPa is taken as a typical pressure difference at the initiation of dyke propagation (Popov, 1973; Stasiuk et al., 1993). After some evolution of the conduit this pressure difference can increase due to the difference between the lithostatic pressure of the country rocks and the hydrostatic pressure of the magma column in the conduit. Foaming and fragmentation of magma in the conduit decreases its density and so can increase total static pressure difference up to several hundreds of MPa. Real dynamic values are less because of friction and acceleration losses. This driving pressure difference allows large velocities and mass discharge rates of magma. In a steady regime the flow is mostly compensated by the hydraulic resistance of the conduit.

In constructing hydrodynamical models of magma flow, instead of using the pressure at the entrance of the conduit p_0, it is convenient to define an excess pressure p_{ex} as the difference between p_0 and the hydrostatic pressure of magma without bubbles:

$$p_{ex} = p_0 - \rho_l g H \quad (2)$$

In Eq. 2 H is the magma chamber depth (length of the conduit); g is gravity acceleration and ρ_l is magma density. The hydrostatic pressure of the magma column is in most cases less than the lithostatic pressure. The typical average densities for a crustal section near the Avachinsky volcano in Kamchatka are illustrated in Fig. 1. So p_{ex} can be much more than 20 MPa at the beginning of an eruption and can be negative at its end due to the low density of the gas–magma mixture. If the magma chamber walls are quite rigid and stable p_{ex} could change from +100 MPa to −200 MPa. In practice the range is expected to be less, approximately from +40 to −40–60 MPa.

2.3. Flow structure in a conduit

Two-phase gas–liquid flow structures have been studied in detail as applied to water–vapor mixtures, oil with gas, and industrial mixtures in chemical technology (e.g. Deich and Philippov, 1968; Wallis, 1969; Boothroyd, 1971; Sternin, 1974; Nigmatullin, 1987). However, in all these cases flow parameters are quite different from those of magma flows, and corresponding results should be applied to magma flow with considerable caution.

Magma has the following specific features: high viscosity of the liquid phase; large difference in density between the condensed and gaseous phases at all pressures; large differences in the

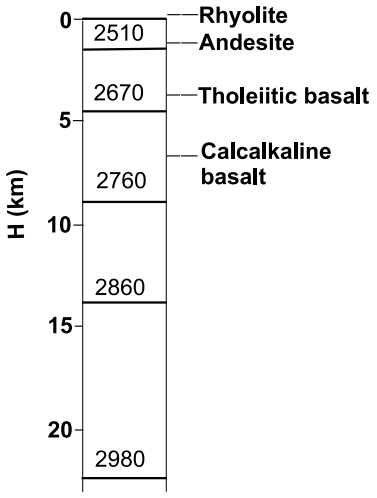

Fig. 1. Average density of crustal layers for different depths in the region of the Avachinskaya volcano group calculated using data of Zubin and Kozyrev (1989). To the left is the depth scale in km; numbers in the middle above the horizontal lines are the values of the average density (kg/m^3) of the crustal layer; to the right the levels are marked where the average densities of the overlying layers are equal to the typical densities of magmas with named compositions (after Murase and McBirney, 1973). Magma of the named composition and indicated density can reach ground surface by hydrostatic forces if sourced from beneath the marked level.

physical and chemical nature of the condensed and gaseous phases; small mass fraction of the volatile components (a few percent); increase of viscosity of the non-volatile component due to volatile exsolution; heterogeneous bubble nucleation on a large number of centers; and large vertical length of the conduit. There are some unique features of flow structures in a volcanic conduit. Rising magma bubbles can reach the state of close packing without bubbles moving relative to the liquid; the transition of a liquid with bubbles into the state of a *foam* is possible. A dispersion of solid particles in gas (gas–pyroclastic flow regime) can develop directly from a magmatic foam. The transition between plug flow and annular flow is not usually expected, except for some types of Hawaiian eruption (Vergniolle and Jaupart, 1990).

There is a flow structure, named 'partly destroyed foam' by Slezin (1980a, 1995a,b), which has not been considered in previous eruption models. In this regime both phases of the two-phase, two-speed flow are continuous. Gas moves through the interconnected pores in a partly destroyed foam faster than the permeable foamy magma. Such permeable systems in silicate melts have been experimentally studied by Eichelberger et al. (1986), Letnikov et al. (1990), Letnikov (1992) and Balyshev et al. (1996). A sharp direct transition from bubble flow to gas–pyroclastic mixture is often assumed. This sharp transition was supposed to result from increasing pressure within bubbles due to pushing viscous melt through thin films dividing bubbles needed for further bubble growth (Sparks, 1978). In fact, an expanding bubble in a close-packed ensemble is surrounded by a foam medium which is deformed not by pushing of viscous liquid through thin films, but with stretching and bending of those films. This stretching and bending becomes easier when films become thinner, and the resistance of the foam to deformation become lower (I.I. Goldfarb, private communication). Graton (1945) wrote that a magmatic foam should be treated as a new phase, but his advice was forgotten. The problem is to describe partly destroyed foam analytically. Here it is approximated by a mass of loose particles partly stuck together. The empirical formulas of Nigmatullin (1987) can be applied to the dynamics of gas flow in loose fills.

There can be from two to four successive zones (Fig. 2) with different flow structure in a volcanic conduit for steady flow. The changes of structure result from the increase of volume fraction of gas. In an homogeneous zone (zone 1) there is only silicate liquid in the conduit. In a bubble zone (zone 2) there is gas–liquid dispersion flow in which liquid is the continuous phase. At large volume concentrations of bubbles ($>50\%$) this can be defined as a foam. In zone 3 three cases are possible, two of which are illustrated in Fig. 2a,b. First, the increase of gas volume during ascent results in the increase of gas bubble sizes. Their upward speed through the liquid results in coalescence due to bubbles overtaking one another (zone 3 in Fig. 2a). Second, the increase of gas volume during ascent results in the gas bubbles growing 'in situ' and rising only with the liquid (Fig. 2b). Bubbles eventually make a foam that can disrupt and create a porous permeable substance of partly destroyed foam through which

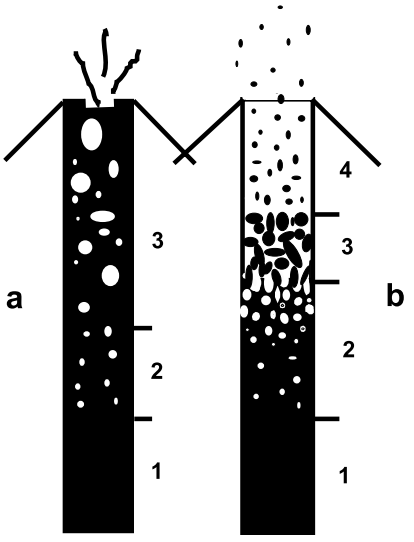

Fig. 2. Possible structures of two-phase flow in a volcanic conduit. (a) The discrete gas separation (DGS) regime: Zone 1, magma without bubbles; Zone 2, single-velocity bubbling flow; Zone 3, DGS (two-velocity bubbling) flow. (b) The dispersion (steady-jet) regime: Zone 1, magma without bubbles; Zone 2, bubbling single velocity flow; Zone 3, partly destroyed foam (PDF, porous, channeled medium); Zone 4, gas–pyroclastic dispersion flow.

gas escapes without entraining particles (Slezin, 1979, 1980a). This structure can be illustrated by pumice, in which most pores are interconnected (Witham and Sparks, 1986). Third, the zone of partly destroyed foam is reduced to zero and the particles become fluidized after fragmentation, provided that the flow velocity and the melt viscosity are both large enough. In dispersed flow (zone 4) the continuous phase is gas and particles are the dispersed phase, behaving typically as solids on the time scale of the flow. A relatively large zone containing a dense gas–pyroclast mixture (a zone of fluidized flow) is a characteristic feature of conduit flows.

Three of the zones have liquid as the continuous phase, and the liquid viscosity is responsible for flow resistance. These three zones are treated as one zone of *liquid flow* that is separated from the zone of *gas–pyroclast flow* by the *fragmentation level*. Volcanic two-phase flows differ from similar flows in technical systems because of the very sharp decrease of resistance at the fragmentation level. The average flow resistance in gas–pyroclast mixtures per unit length of conduit is at least 5–6 orders of magnitude less than the flow resistance in a zone of liquid flow. In the gas–pyroclast zone gravitational forces are large and inertial forces are very small.

2.4. Classification of eruptions based on flow structure

Slezin (1979, 1995a) proposed a classification of the basic eruption regimes on the basis of flow regimes (two-phase flow structure) at the conduit exit.

(1) Liquid with gas in the form of separated bubbles appears at the surface. The *discrete gas separation* (DGS) regime can take place only if bubble sizes are large enough for their speed to be much greater than the speed of liquid. This regime corresponds to all eruptions with gas emission in discrete portions, including nearly pure effusive and nearly pure explosive (Strombolian) activity. Observations at Tolbachik (1975–1976) show that during Strombolian activity gas emission on average is directly proportional to magma discharge rate (Slezin, 1990).

(2) A continuous eruption of gas–particle flow appears at the surface. The *dispersion regime* corresponds to all gas–pyroclast eruptions including high intensity, catastrophic explosive eruptions (CEE). In this regime two different zones of liquid flow and of gas–pyroclast flow exist in the conduit, separated by the *fragmentation level*. The possibility of major changes of total flow resistance after very small displacements of this boundary make such flows unstable and make possible sharp and unexpected changes in the eruption character and intensity.

(3) A two-phase medium erupts in which both phases are continuous and move with different velocities. This medium consists of high viscosity magma with a system of interconnected pores and channels, through which gas rapidly escapes. This regime is named the *regime of partly destroyed foam* (PDF). The third regime corresponds to extrusive eruptions. This is possible only as a very slow movement of high viscosity magma, such as in lava dome eruptions.

3. Conditions for the basic regimes of volcanic eruptions

The boundaries between the three flow regimes are defined on the basis of six main parameters for conduit flow (Slezin, 1979, 1995a): magma ascent velocity, melt viscosity, number of bubble nuclei per unit volume of magma, mass fraction of volatile components, volatile solubility coefficient and mean size of the pyroclastic particles. They depend on many properties of the magma and the eruption system. For example, mean size, porosity, and the shape of the particles can depend on some small constituents modifying surface properties of magma (Kovalev and Slezin, 1979a,b). The number density of bubble nuclei depends on many factors, including volatile content, composition of melt, temperature and speed of decompression.

3.1. Discrete gas separation and dispersion regimes

For the fragmentation of magma foam a relatively large volumetric fraction of gas bubbles

should be attained near the state of close packing. At close packing, the interbubble melt films become thin and unstable enough for disruption to begin due to further foam expansion. The films' stability depends not only on the volumetric fraction of gas, but also on the small amounts of some magma components known as 'foam stabilizers' (Kovalev and Slezin, 1979a,b). So the foam density before disruption can vary between different magmas.

The attainment of the close-packed state can be prevented by either low gas content (<0.06 wt%) or gas removal by rising bubbles. The latter is plausible, provided the primary bubbles are able to overtake and coalesce with one another, in the 'discrete gas separation' regime. The necessary condition for this can be written as follows:

$$\Delta l > k_1 d \tag{3}$$

where d is the mean distance between bubbles; $\Delta l = l_L - l_S$ is the difference between the paths traveled by large (l_L) and small (l_S) bubbles as they rise through the melt, and k_1 is a coefficient accounting for the non-uniform distribution of bubbles in space. The distance between the bubbles is no larger than the distance between their centers:

$$d < n^{-1/3} \tag{4}$$

where n is the number of bubble nuclei in a unit magma volume. The value of n is taken as constant after a very short nucleation interval (Toramaru, 1989). The nucleation of new bubbles is most likely at the greatest distance from existing bubbles where maximum supersaturation is expected (Blower et al., 2001). Consequently, by the end of nucleation the distribution of the bubble nuclei in space must be approximately uniform, and we can put:

$$k_1 = 1 \tag{5}$$

The path, $\bar{l}$, traveled by the bubble as it rises at speed $\bar{u}$ relative to magma, can be approximately defined as:

$$\bar{l} = \bar{u}T \tag{6}$$

T is the time of bubble rise. If it does not coalesce with its neighbors each bubble can grow to a maximum close-packing size, approximately equal to $n^{-1/3}$. Then the average speed relative to magma, defined approximately as an arithmetic mean of the initial and the final rate, is:

$$\bar{u} = \frac{\rho_l g}{36\eta} n^{-2/3} \tag{7}$$

where ρ_l is the liquid density, g is the acceleration of gravity, and η is the liquid viscosity.

A bubble can rise through magma during the time T that magma takes to rise from the level of the bubble generation h_0 to the level h_p, where a close-packing state is attained. Here the ratio between the gas and liquid volumes V_g/V_l becomes approximately 3. Expressing the difference between the levels through a pressure difference $(p_0 - p_p)$:

$$h_0 - h_p = \frac{p_0 - p_p}{\overline{\rho} g + G\dfrac{\overline{U}\eta}{b^2}} \tag{8}$$

Here $\overline{\rho}$ is the average density of the melt–bubble mixture, and $\overline{U}$ is the average flow velocity on the $h_0 - h_p$ interval, b is the characteristic cross-dimension of the conduit and G is the factor characterizing its cross-sectional geometry. The time T can be found as the distance $h_0 - h_p$ divided by $\overline{U}$:

$$T = \frac{p_0 - p_p}{\overline{U}\overline{\rho} g + G\dfrac{\overline{U}^2\eta}{b^2}} \tag{9}$$

From continuity of the flow we get:

$$\overline{U}\overline{\rho} = U\rho_l, \quad \overline{U} = \frac{U\rho_l}{\overline{\rho}} \tag{10}$$

where U and ρ_l are the flow speed of magma without bubbles and its density, respectively. The value of $\overline{\rho}$ (and hence of $\overline{U}$) over the distance $(h_0 - h_p)$ can be calculated assuming equilibrium for volatiles between liquid and gas phases. For typical volatile contents, the ratio $\overline{U}/U$ ranges between 2.5 and 1.7 and is equal to 2 with a volatile content of slightly less than 5%. Putting $\overline{U} = 2U$ in Eq. 9 and taking into account Eq. 10, we obtain:

$$T = \frac{p_0 - p_p}{U\rho_l g}\left(1 + G\frac{4U\eta}{g\rho_l b^2}\right)^{-1} \tag{11}$$

The pressures p_0 and p_p can be found from the

magma volatile content, c_0, and Henry's law (Eq. 2). Assuming the gas to be ideal, one can write:

$$\frac{V_g}{V_l} = \frac{\rho_l p_a (c_0 - a\sqrt{p})}{\rho_{ga} p} \tag{12}$$

where p_a is atmospheric pressure and ρ_{ga} is the gas density at this pressure and magma temperature. $V_g/V_l = 0$ at p_0 and $V_g/V_l = 3$ at p_p. Substituting these values into Eq. 11 and then substituting Eqs. 11 and 7 into Eq. 6, we can find the distance that an average bubble can rise relative to magma $l = \bar{l}$.

Let us define the 'large' and the 'small' bubble and express Δl through $\bar{l}$. The radii of large and small bubbles (r_L and r_S, respectively) are chosen so that the probability that the 'small' bubble is ahead of the 'large' bubble in the 'capture zone' is unity in any conduit cross section after nucleation ceases. The capture zone is assumed to be a vertical circular cylinder with the same radius as the 'large' bubble. This approximation is based on the tendency of small bubbles to follow flowlines around large bubbles, but neglects coalescence.

The probability calculation indicates that, for typical conduit widths, any number of bubble nuclei per unit volume and any bubble size distribution, we can use the maximum radius r_{max} for the 'large' and the minimum radius r_{min} for the 'small' bubble. For instance, for a uniform size distribution ($dN(r)/dr = $ Constant between r_{min} and r_{max}), the condition that the probability of at least one pair of a 'small bubble ahead of a large bubble in the capture zone' in any cross section of the conduit is unity is as follows:

$$\Delta r\, r_L > \frac{\Delta r_{max}}{\sqrt{6S}} n^{-2/3} \tag{13}$$

where $\Delta r = r_{max} - r_L = r_S - r_{min}$, $\Delta r_{max} = r_{max} - r_{min}$, and S is the cross-sectional area of the conduit. For example, let $S = 100$ m^2, $\Delta r_{max} = 50$ μm-5 μm$ = 4.5 \times 10^{-5}$ m, and $n = 10^{11}$ m^{-3}. Then Eq. 13 is rewritten as:

$$\Delta r\, r_L > 8.5 \times 10^{-14} \text{ m}^2 \tag{14}$$

Because $r_L < r_{max} = 5 \times 10^{-5}$ m, the condition necessary for Eq. 14 to be valid is $\Delta r > 1.7 \times 10^{-9}$ m. That is, r_L can differ from r_{max}, and r_S from r_{min}, by not more than a hundredth of a percent.

The bubble size distribution depends on the kinetics of bubble nucleation and growth. After initial nucleation, oversaturation can decrease due to further nucleation, and gas diffusion into existing bubbles. The competition of these two processes involves a rapid cessation of nucleation and the stabilization of the number of bubbles in a unit mass of magma. Theoretical calculations indicate that the nucleation interval is of the order of 0.1 MPa (Toramaru, 1989). My approximate estimates gave values of about 1 MPa, that is less than 1% of the total pressure difference in the conduit. The initial bubble size distribution is thus formed, which changes during further rise of magma due only to bubble growth. New bubble nuclei can be generated if the pressure decrease accelerates, probably in the last stages of magma ascent when the melt–bubble mixture is near to close packing, and is not expected to play a significant role in controlling the flow regime.

Bubble growth in ascending magma proceeds by two mechanisms: mass diffusion and decompression. Some time after the end of nucleation the first mechanism prevails, but soon its influence becomes unimportant. Sparks (1978) showed these effects for a single bubble; for a bubble growing in an ensemble of other bubbles they should be more prominent. The effect of the diffusion depends on the dynamics of magma ascent and tends to restrict the bubble size range; decompression tends to keep the ratio of the bubble radii constant. Hence, if there is no coalescence, the change of the ratio of the largest and smallest bubble sizes should be small, and its value, measured in pyroclastic particles, should give the lower limit of this ratio in the conduit.

The measurement of bubbles in pyroclastic particles (Heiken and Wohletz, 1985) and in Tolbachik scoria (the bubbles whose form suggested a coalescence origin were discarded) gave $r_{max}/r_{min} \sim 10$. Obviously, this ratio cannot be smaller in the conduit. Considering the above estimates one also can put $r_L/r_S \sim 10$. Since $l \sim r^2$, one can put approximately $\Delta l = l_L - l_S \sim l_L$, and also $r_L \sim 2\bar{r}$ and $l_L \sim 4\bar{l}$. Consequently:

$$\Delta l = 4\bar{l} \tag{15}$$

Taking into account Eqs. 5, 6 and 15, the starting condition 3 can be rewritten as:

$$\bar{l} > \frac{1}{4} n^{-1/3} \tag{16}$$

The value of $\bar{l}$ can be found using Eq. 6 through the substitution of Eqs. 7 and 11 into it. Performing appropriate substitutions in Eq. 16 and simple manipulations, we obtain the condition necessary for the discrete gas separation regime:

$$U \eta n^{1/3} \frac{a^2}{c_0^2} F(Q)(1 + F_1) < 0.11 \tag{17}$$

where

$$F(Q) = \left(1 - Q^2 \left(\sqrt{1 + \frac{2}{Q}} - 1\right)^2\right)^{-1},$$

$$Q = \frac{\rho_l p_a a^2}{6 \rho_{ga} c_0}, \quad F_1 = 4G \frac{U \eta}{g \rho_l b^2}$$

All quantities that enter the expression for Q, except c_0, have a possible variation range of 20–30%; c_0 may vary several-fold. My estimate suggests that Q varies within 0.05–1, with $F(Q)$ varying only two-fold (1.08–2.15). Considering the general validity of this derivation and the accuracy of the initial parameter values, $F(Q)$ can be replaced safely by 1.6 as a typical value.

The quantity F_1 is a ratio between the contributions of friction and magma weight to the pressure loss over the interval of the bubble flow. In the discrete gas separation regime, when the zone of liquid suspended in gas is absent, its value is always smaller than one and is approximately $(\rho_l - \bar{\rho})/\rho l$, where $\bar{\rho}$ is the average density of magma in the conduit. Near the boundary between the discrete gas separation and dispersion regimes $F_l < 0.5$; it tends to this value only if all the conduit is filled with a bubbling liquid and its length is small. Taking the maximum value F_1 and putting it into Eq. 17, together with the average value of $F(Q)$, we obtain the inequality:

$$Di = U \eta n^{1/3} \frac{a^2}{c_0^2} < 0.05 \tag{18}$$

The dimensionless number Di (Slezin, 1979, 1995a) has a critical value $Di_{cr} = 0.05$. When $Di < 0.05$ the discrete gas separation regime occurs; when $Di > 0.05$ one of two other regimes (dispersion or extrusive) is possible. Slezin (1979, 1995a) proposed that the condition $Di > Di_{cr}$ is necessary, but not sufficient, for the dispersion regime.

A change to the dispersion regime is promoted by the increase of magma ascent velocity, viscosity, and the number of bubble nuclei per unit mass. Less obvious is the dependence upon the volatile content and the solubility coefficient a. Both the increase of the volatile content and the decrease of solubility result in the appearance of bubbles at a greater depth, lengthening their floating time, and, accordingly, increasing the probability of their coalescence and the rapid removal of large gas volumes from the flow. This criterion can be used where the magma volatile content is sufficient for the bubbles to attain close packing at least at atmospheric pressure, and this condition holds for typical gas contents ($c_0 > 0.0006$).

Let us consider the variables that control the Di criterion more generally. Velocity U can be treated as a dynamic parameter. The volatile content, c, characterizes the main components of the system that control the flow dispersion. The other variables, η, n, and a, describe system properties, mainly of magma. They enter the Di criterion as co-factors and because they vary unidirectionally, as magma changes from basic to silicic, the combination

$$\xi = \eta n^{1/3} a^2 \tag{19}$$

can be taken as a generalized characteristic of magma, and Di can be written as a function of three variables:

$$Di = \frac{U \xi}{c_0^2} \tag{20}$$

where $\xi \sim 10^{-2}$ s m^{-1} for silicic magma, and $\sim 10^{-5}$ s m^{-1} for basic magma.

After substituting Di_{cr} for Di in Eq. 20, we obtain an equation connecting three variables U, ξ and c_0, which describes a curved plane. All the points below this plane represent combinations of parameters corresponding to the discrete gas sep-

aration (DGS) regime. Some cross sections of this curved plane for constant values of ξ are shown in Fig. 3. The DGS regime should prevail when basic magmas erupt, but has a very small probability for silicic eruptions.

Magma ascent velocity U is a convenient variable to investigate evolution of eruptions. Consequently, the condition for the realization of the DGS regime can be defined as:

$$U \leq U_{cr} = \frac{Di_{cr} c_0^2}{\xi}, \quad Di_{cr} = 0.05 \tag{21}$$

Wilson and Head (1981) made their calculations of bubble rise and coalescence for basalt magmas, using the magma velocity as the only governing parameter on the evolution of an eruption. Their results are in good agreement with the results obtained using formula Eq. 21.

3.2. Dispersion and PDF (extrusive) regimes

When $Di > Di_{cr}$ the state of close packing is reached due to bubble growth in the ascending magma, and produces foam, which begins to disrupt. To create the dispersion regime this disruption must be complete, and the velocity of the discharged gas flow must be sufficient for fluidization of the resulting particles. In a steady flow immediately after the beginning of foam disruption these conditions as a rule are not fulfilled. Foam disrupts only partly. A porous substance (partly destroyed foam) is formed. This is justified by the interconnected character of pumice (Wittam and Sparks, 1986; my own measurements in basaltic slags of Tolbachik), and by the permeable nature of extrusive domes (Sparks et al., 2000).

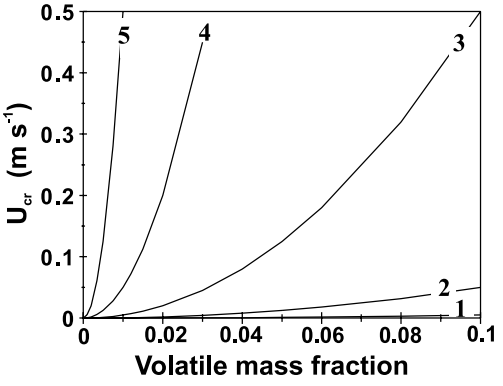

Fig. 3. Critical velocity of magma ascent plotted against volatile content. Curves labeled from 1 to 5 describe critical velocities of magma ascent against volatile content, c_0, corresponding to ξ values from 10^{-1} to 10^{-5} s m^{-1}, respectively. For a given value of ξ the DGS regime plots to the right of and below the curve of critical velocity.

With further magma ascent, the volume flow rate and the velocity of gas increase, and fluidization and transformation of the foam to a gas–pyroclast mixture can occur. To describe the process of gradual foam disruption I treat the partly destroyed foam as a mass of separate particles characterized by definite sizes and partly stuck together (Slezin, 1980a, 1995a,b). Gas can flow through the channels between particles and fluidize them if it has sufficient velocity not only to suspend them, but also tear them from each other. If the gas velocity is not sufficient for particle fluidization even at the exit of the conduit, partly destroyed foam (PDF) extrudes.

The gas velocity needed for fluidization depends on the particle size, density, and on the sticking forces. The magnitudes of the sticking forces are not known, so we must consider several possible cases. The particle size distribution forms in the process of foam disruption, and is assumed to change little in the gas suspension. Particles should be smaller when viscosity of magma is larger and eruption is more intensive because of both larger pressure gradients and more brittle response of magma due to faster deformation. These factors also lead to larger pressures in bubbles before disruption. As a limit, pyroclasts can consist only of 'shards' that are remnants of interbubble walls. The density of shards is ρ_l, but they have complicated shapes and large drag coefficients in the gas flow. Larger particles include pores and their density is less than ρ_l, but their shape is more isometric and the drag coefficient is not so large (Wilson and Huang, 1979). In further calculations a polydispersed particle suspension was substituted by a monodispersed one (Slezin, 1980b), consisting of particles with an appropriate density and with a drag coefficient equal to unity in agreement with experiments (Walker et al., 1971).

The volume fraction of free gas needed for flu-

idization δ_0 equals 0.4 for spheres (Boothroyd, 1971). A similar value (0.44) was measured on ash from Bezymyanny volcano (Alidibirov and Kravchenko, 1988). The dispersion regime begins when fluidization conditions are fulfilled at the vent exit into the air at pressure p_a (atmospheric) and gas density ρ_{ga}. Assuming that all gas has been exsolved, the required speed can be found from the continuity condition:

$$u_g = \frac{U\rho_l c_0}{\rho_{ga}\delta_0} \tag{22}$$

The speed of the particles u_p can be found as a difference between u_g and the terminal speed u_t of the particles of average size d_p:

$$u_t = \sqrt{\frac{4g\rho_p d_p}{3\rho_{ga}}}k(\delta_0) \tag{23}$$

The subscript p is used with the variables that characterize the particles, and $\rho_p = \rho_l(1-\beta)$, where β is the porosity of particles. The 'flow tightness' (i.e. the influence of adjacent particles) is taken into account by multiplying the expression by the coefficient $k(\delta)$. The speed of the particles in a stable flow must satisfy the continuity condition for non-volatile components:

$$u_p = \frac{U\rho_l}{\rho_p(1-\delta_0)} \tag{24}$$

Denoting the gas speed sufficient to surpass the cohesion of the particles as $u(F_p)$, where F_p is the cohesive force needed to tear one particle from another, the condition for the dispersion regime can be written as:

$$u_g \geq u_p(\delta_0) + u_t(\delta_0) + u(F_p) \tag{25}$$

The three terms on the right hand side of Eq. 25 are not equivalent. The second term depends on the size and density of the particle only, but the first term depends on the magma upward velocity U and is in nearly all cases much less than the second term. The third term cannot be estimated: it could be much smaller or much larger than the second term. So, as a first approximation we neglect the first term and consider possible limiting cases for the third term.

Assuming that the first term in the right side of Inequality 25 is equal to 0 and substituting in it Eqs. 22–24, then:

$$U \geq \frac{\delta_0\rho_{ga}}{\rho_l c_0}\left(\sqrt{\frac{4g\rho_p d_p}{\rho_{ga}}}k(\delta_0) + u(F_p)\right) \tag{26}$$

If the cohesive force is much less than the force needed for fluidization of loose particles, and the particles are not stuck together after disruption, we can put $u(F_p) = 0$ and rewrite Eq. 25 as:

$$U \geq \frac{\delta_0 k(\delta_0)}{c_0}\sqrt{\frac{4g\rho_{ga}(1-\beta)d_p}{3\rho_l}} \tag{27}$$

If the cohesive force is much larger than the force needed for fluidization we can write:

$$U \geq \frac{\delta_0\rho_{ga}}{\rho_l c_0}u(F_p) \tag{28}$$

If condition 26 or one of the conditions 27 and 28 is not fulfilled, the PDF regime can take place. Illustrative values corresponding to the moment of fluidization at the exit in Eq. 27 are: $\delta_0 = 0.44$; $k(\delta_0) = 0.1$ (Alidibirov and Kravchenko, 1988), $\rho_l = 2500$ kg m^{-3}, $\rho_{ga} = 0.2$ kg m^{-3} and $\beta = 0.5$. As a result we obtain:

$$U \geq \frac{0.0017}{c_0}\sqrt{d_p} \tag{29}$$

where d_p is in m and U in m s^{-1}. Substituting in Eq. 29 values of c_0 about 0.05 and $d_p = 10^{-4}$–10^{-2} m, we find that, if particles do not stick to each other, for the extrusive regime to be realized the velocity of magma ascent should be about 0.001 m s^{-1} or less. Magma ascent velocities corresponding to the extrusive regime on Mount St. Helens (Slezin, 1991, 1995a) give values of more than 0.001 m s^{-1}. So the effect of cohesion of particles may be not small. Equating the drag force and F_p, an expression for $u(F_p)$ is obtained through F_p and an approximate inequality analogous to Eq. 29 is found:

$$U \geq \frac{0.00012}{c_0}\frac{\sqrt{F_p}}{d_p} \tag{30}$$

The cohesive force F_p increases when the particle size d_p increases, so the dependence of the right hand side of Eq. 30 as well as the right

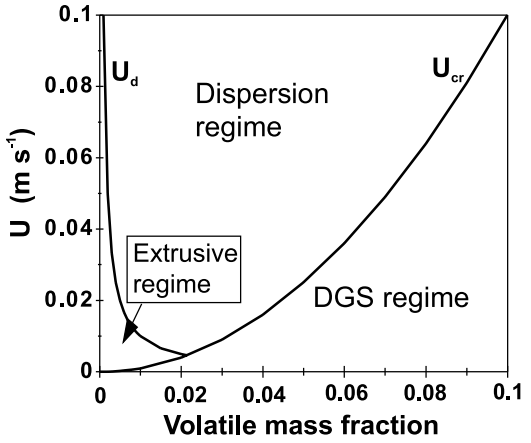

Fig. 4. Map showing eruption regimes on a plot of magma velocity versus volatile (water) content bounded by critical curves. The curve for U_{cr} divides the DGS regime from others, calculated using Eq. 21 with $\xi = 5\times10^{-3}$ s m^{-1}; curve U_d divides extrusive and dispersion regimes calculated using Eq. 31 with $A = 0.01$.

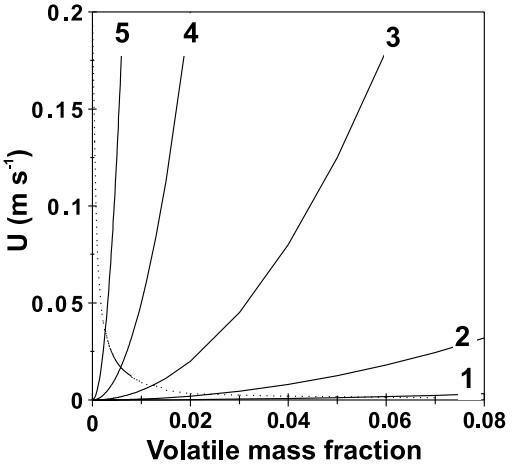

Fig. 5. The dependence of eruption regimes on the parameter ξ. Other parameters are the same as in Fig. 4. Curves with numbers from 1 to 5 correspond to the values of ξ from 10^{-1} to 10^{-5} s m^{-1}, respectively (from rhyolites to basalts). For a given value of ξ the DGS regime plots to the right of and below the curve of critical velocity. The dispersion and extrusive regimes plot above the curve (see Fig. 4).

hand side of Eq. 29 on d_p is not strong. So for an approximate estimate one can write instead of Eqs. 29 or 30:

$$U_d = \frac{A}{c_0} \tag{31}$$

where U_d is in m s^{-1} and A can be from $\sim 10^{-5}$ m s^{-1} for the small, non-cohesive particles to $\sim 10^{-3}$ m s^{-1} for the case when the cohesive force is greater than particle weight.

3.3. Relations between three basic regimes

The conditions for each basic regime are summarized in Table 1 and illustrated in Fig. 4. For the small non-cohesive particles, the curve U_d would be lower than is shown in Fig. 4; when the particle cohesive force is large, the curve could be much higher. The curve U_{cr} can have different inclinations (Fig. 5). In principle any regime can be realized for any magma (Fig. 5), but the relative probabilities of the regimes are quite different. For basalt eruptions the DGS regime prevails; the dispersion regime can be realized only when the volatile content is small and the speed of magma ascent is large; and the PDF regime cannot practically be realized. For silicic eruptions the dispersion regime strongly prevails; the PDF (extrusive dome) regime is feasible for a wide range of parameters, but the DGS regime has very low probability. All this corresponds well to observations.

Table 1
The conditions necessary for different regimes to occur

Condition: Regime	$U > U_{cr}$	$U < U_{cr}$	$U > U_d$	$U < U_d$
DGS	–	+	0	0
PDF	+	–	–	+
Dispersion	+	–	+	–

'+' means the condition must be fulfilled; '–' means the condition must not be fulfilled; '0' means the condition is not critical.

Table 2
Average values of the parameters typical for the Tolbachik eruption in 1975–1976

	U (m s$^{-1)}$	η (Pa s)	n (m^{-3})	c_0	a (Pa$^{-1/2}$)	d_p (m)	ρ_p (kg m^{-3})
Northern Breakthrough	0.15	10^5	3×10^{10}	0.09	3×10^{-6}	0.01	1500
Southern Breakthrough	0.02	10^3	3×10^{10}	0.01	3×10^{-6}	–	–

3.4. Some estimates for well known eruptions

3.4.1. Tolbachik 1975–1976

This eruption is described in a monograph (Fedotov, 1984). It includes two stages that were named the *North* and *South Breakthrough*. These stages differ from each other both in time and in space (10 km distance) and in regime. At the South Breakthrough there was only the DGS (classic Strombolian) regime. At the North Breakthrough the dispersion regime mostly occurred and was very stable for several days. Some average characteristics of both stages are shown in Table 2. For the South Breakthrough $Di = 0.005$ was obtained, which is an order of magnitude less than the critical value and corresponds to the stable DGS regime. For the North Breakthrough $Di = 0.1$, which corresponds to the dispersion regime. In the latter case the value of Di is only a little greater than critical, and instability of mass discharge rate related to changing regimes can be expected. Such an instability was observed near the end of the North Breakthrough eruption.

3.4.2. Mount St. Helens 1980

The first stage of the Mount St. Helens eruption included mild phreatic explosions and deformation of the volcanic edifice (Lipman and Mullineaux, 1981). Then a large landslide triggered a directed blast. A gas–pyroclast steady-jet stage followed, which lasted for 9 h in the stable regime and then stopped abruptly. After a 3.5 week pause a dome started to extrude. During the steady-jet (Plinian) phase 0.25 km^3 of juvenile dense magma with a density of 2600 kg m^{-3} was erupted, so the average volume discharge rate was about 8000 m^3 s^{-1} (Carey et al., 1990). At the beginning of the extrusive dome growth the volume discharge rate was about 8 m^3 s^{-1} (Swanson and Holcomb, 1990). Slezin (1991) estimated the magma ascent velocity during the steady-jet stage and consequently the conduit cross-sectional area using characteristics of the gas–pyroclastic jet and the theoretical model described in the next section. This velocity was a little more than 1 m s^{-1}. So the magma ascent velocity during the extrusive stage should be about 0.001 m s^{-1}.

The original content of the dissolved water in the melt phase of the magma, calculated using mineral-phase relations, was $c_0 = 0.046$ (Rutherford et al., 1985). Using granulometric data and space-size distribution of pyroclastics from Sarna-Wojcicki et al. (1981), the average size of particles (total volume divided by the total number of particles) was estimated as $d_p = 0.001$ m. Substituting appropriate values in Eq. 21, we find that U_{cr} is much less than 1 m s^{-1} with any feasible value of ξ for Mount St. Helens magma. The theory predicts the dispersion regime. Calculation of U_d, dividing the dispersion and PDF regimes (Eq. 29), yields 0.0007 m s^{-1}, which is similar to observations on the dome growth (Moore et al., 1981).

3.4.3. Bezymyanny 1956

The eruption of Bezymyanny 1956 followed the same scenario as Mount St. Helens 1980 (Belousov and Bogoyavlenskaya, 1988). Quantitative data are not so detailed as for Mount St. Helens. The dissolved water content is between 0.05 and 0.06 (Kadik et al., 1986) and the average particle size is approximately the same as on Mount St. Helens. Hence the value of U_d must also be the same. The average magma discharge rate during the first 3 months of dome extrusion was 3 m^3 s^{-1}. The observations on Bezymyanny also confirm theoretical results.

4. Theory of the dispersion regime

4.1. Formulation of the problem and solution method

4.1.1. Physical formulation

The problem is as follows: magma flow moves through a vertical conduit under a certain pressure difference between its ends. The eruption type, mass discharge rate, flow structure, and velocity of the flow at the exit of the conduit must be found for any combination of system parameters. In the dispersion regime there are both main forms of two-phase flow in a volcanic conduit: liquid and gaseous (gas–pyroclast mixture). The following simplifying assumptions were made: (1) flow is steady-state, isothermal and one-dimensional; (2) mass and momentum exchange between phases is an equilibrium process; (3) the gas–pyroclast mixture is monodisperse and non-colliding; (4) the density of the condensed phase is independent of the dissolved volatile content; (5) the condensed phase is incompressible and the gas is ideal; (6) nucleation of bubbles starts at gas saturation conditions and stops after a very small interval of time, which is neglected, and then the number of bubbles per unit mass remains constant.

4.1.2. The system of equations

The mathematical description of conduit flow includes: (1) equations describing conservation laws: for the mass of each component, momentum and energy; (2) equations of state for each phase and for the mixture; (3) equations describing interaction between phases: mass, energy and momentum exchange. Boundary conditions are required at the ends of the conduit and the conditions on the boundaries between zones with different flow structure.

Assumptions of isothermal flow and impermeability of the conduit walls for heat and matter allow equations of energy conservation and ones describing energy exchange between phases to be neglected. In its general form the systems of equations, with simplifying assumptions, can be written as:

$$(\rho u)_{nv} = \text{Const} \tag{32a}$$

$$(\rho u)_{v} = \text{Const} \tag{32b}$$

$$\mathrm{d}p = \mathrm{d}p_{st} + \mathrm{d}p_{u} + \mathrm{d}p_{d} \tag{33}$$

$$\rho_g = \rho_g(p) \tag{34a}$$

$$\rho_l = \rho_l(p) \tag{34b}$$

$$\rho = \rho(p, \rho_g, \rho_l) \tag{34c}$$

$$c = ap^{1/2} \quad \text{at } p < \frac{c_0^2}{a^2} \tag{35a}$$

$$c = c_0 \quad \text{at } p \geq \frac{c_0^2}{a^2} \tag{35b}$$

$$u_g - u_l = F(P_i) \tag{36}$$

In the equations, p is pressure, u is velocity, and ρ is density; when used without subscripts these quantities relate to the two-phase mixture as a whole; c is dissolved volatile component content in the condensed phase; c_0 is total volatile content; a is the gas solubility constant; P_i are parameters of the flow on which momentum exchange between phases depends. Subscripts st, u, and d are used to describe static, dynamic and dissipative pressure losses, respectively; nv describes the non-volatile component; v describes the volatile component; g refers to the gas phase; and l to the condensed (liquid) phase.

Eqs. 32 are continuity equations; Eq. 33 is the equation of momentum written as a balance of pressure increments and describes the change of pressure along the conduit; Eqs. 34 are the equations of state for each phase and for the mixture; Eqs. 35 describe mass exchange between phases (solubility of the volatile component in the melt); Eq. 36 characterizes momentum exchange between phases. Specific forms of the equations depend on the flow structure and are not the same in the different parts of the conduit. Equations use real velocities and densities of the phases rather than normalized values. In the zones where all the phases have the same velocity, we write one continuity equation:

$$\rho u = \rho_l U \tag{37}$$

If the velocities of the phases are different in the

zones of partly destroyed foam and dispersion, we write two continuity equations, one for each component:

$$u_l(1-c)(1-\beta)(1-\delta) = U(1-c_0) \tag{38a}$$

$$\rho_g u_g \delta + \rho_g u_l \beta(1-\delta) + \rho_l u_l c(1-\beta)(1-\delta) = \rho_l U c_0 \tag{38b}$$

Here β is the gas volume fraction enclosed within the particles and δ is the volume fraction of free gas in the flow. In Eq. 38b, written for the volatile component, the first term on the left hand side describes the mass flux of free gas, the second term describes the mass flux of gas in the pores of the particles, and the third term describes the mass flux of the volatile component dissolved in the condensed phase. The second term of Eq. 38b is much smaller than the others and in most cases can be neglected.

If the vertical coordinate h, is directed down, and the origin is placed at the exit of the conduit, one can write the terms of Eq. 33 in the following way:

$$\mathrm{d}p_{st} = \rho g \mathrm{d}h \tag{39}$$

$$\mathrm{d}p_u = -\rho_u u \mathrm{d}u \tag{40}$$

The inertial term, Eq. 40, is relevant to the gas–pyroclast zone only, because in other zones it is negligibly small. The third (dissipative) term in the right hand side of Eq. 33 in the region of the liquid flow (i.e. first three zones from the magma chamber) has the form:

$$\mathrm{d}p_d = G\frac{u_l}{\sigma}\mathrm{d}h \tag{41a}$$

$$\sigma = \frac{b^2}{\eta} \tag{41b}$$

where σ is called the conduit conductivity, b is the characteristic cross-dimension of the conduit (for a fissure it is the width, for a cylinder it is the diameter), η is the constant magma viscosity, G is the coefficient relating to the form of the conduit cross section (for a fissure $G=12$ and for cylinder $G=32$).

In the zone of the gas–pyroclast mixture:

$$\mathrm{d}p_d = k_f \frac{u^2}{4R}\rho \mathrm{d}h \tag{42}$$

where k_f is the friction coefficient and R is the conduit radius in cylindrical form. For typical velocities of gas–pyroclast mixtures and conduit radii, k_f depends only on the wall roughness (Chugaev, 1975). Slezin (1982a, 1983) estimated the friction coefficient as 0.02 or a little less.

If temperature is about 1000°C and pressure is no more than a few hundreds of MPa, the melt is an incompressible liquid and the gas is ideal. So the equations of state of the phases are:

$$\rho_l = \mathrm{Const} \tag{43a}$$

$$\frac{p}{\rho_g} = \mathrm{Const} = \frac{p_a}{\rho_{ga}} \tag{43b}$$

where p_a and ρ_{ga} are, respectively, the atmospheric pressure and the gas density at the atmospheric pressure and the temperature of magma.

For the bubbling flow:

$$\frac{1}{\rho} = \frac{c_0-c}{\rho_g} + \frac{1-(c_0-c)}{\rho_l} \tag{44}$$

For the gas–pyroclast mixture and partly destroyed foam:

$$\rho = \rho_g \delta + \rho_p(1-\delta) \tag{45a}$$

$$\rho_p = \rho_l(1-\beta) + \rho_g \beta \approx \rho_l(1-\beta) \tag{45b}$$

The difference between gas and pyroclast velocities can be found from the equation:

$$(u_g-u_l)^2 = \frac{g d_p \rho_l (1-\beta)}{C_f(\delta)\rho_g} \tag{46}$$

where d_p is the diameter of the particle and $C_f(\delta)$ is its drag coefficient. In the dilute gas–particle mixture the drag coefficient is assumed to be 1, in accordance with experimental data of Walker et al. (1971). In the zone of PDF the drag coefficient increases due to high concentration and is estimated using empirical formulae (Nigmatullin, 1987).

4.1.3. Boundary conditions

At the conduit entrance the pressure p_0 was

fixed as the pressure at the top of the magma chamber:

$$p/_{h=H} = p_0 \tag{47a}$$

$$p/_{h=0} = p_{exit} \tag{47b}$$

The pressure p_{exit} is the atmospheric pressure p_a if the flow velocity at the exit is no more than the local sound velocity. If the velocity of the flow rises to this critical value, then a jump-like change of pressure and density arises at the conduit exit. This constitutes the choked flow condition. In this case p_{exit} must be fixed on the inner side of the pressure jump:

$$\begin{array}{ll} p_{exit} = p_a & \text{when } R<R_{cr} \\ p_{exit} = p_a + \Delta p_s & \text{when } R>R_{cr} \end{array} \tag{48}$$

In the latter case the boundary condition depends on the flow characteristics. The pressure jump Δp_s must be set so that the sound velocity on its inner side is equal to the flow velocity. This was done by iteration. Sound velocity in a gas–particle mixture depends on the mass fraction of particles, average particle size distribution, and the sound wave frequency (steepness of the front). The sound velocity was estimated after Deich and Philippov (1968):

$$u_s = \sqrt{\frac{np}{x\rho\left(1+\frac{1-x}{x}\frac{\Delta u_p}{\Delta u_g}\right)}} \tag{49}$$

where n is the exponent in the polytropic (isentropic) law, x is the mass fraction of free gas, Δu_g and Δu_p are the average increments of gas and particle velocities, respectively, after a sound wave front has passed.

The relation $\Delta u_p/\Delta u_g$ in Eq. 49 defines the dependence of the critical velocity on the sizes of particles and wave frequency. The following limit cases are considered: (1) the wave front is very steep and the particles are large; (2) the wave front is gently sloping and the particles are small. In the first case, a passing wave cannot change the particle velocity (cannot pass momentum and energy to large particles), $\Delta u_p \sim 0$, and Eq. 49 is reduced to:

$$u_s^{\max} = \sqrt{\frac{np}{x\rho}} \approx \sqrt{\frac{np}{\rho_g}} \tag{50}$$

In the second case, particles exactly follow the gas motion and they exchange momentum and energy, $\Delta u_p/\Delta u_g \sim 1$ and Eq. 49 is reduced to:

$$u_s^{\min} = \sqrt{\frac{np}{\rho}} \approx \sqrt{\frac{npx}{\rho_g}} \approx \sqrt{\frac{xp}{\rho_g}} \tag{51}$$

In the first case, the critical velocity equals that in a pure gas phase, in the second case it equals the critical velocity in the gas having the same elastic properties, but approximately $1/x$ times larger density.

In Eq. 51 we have put $n \sim 1$, because in a mixture containing a small mass fraction of gas rapid heat exchange between particles and gas allows an isothermal approximation of expansion and compression when a sound wave passes. If in Eqs. 50 and 51 values approximately correspond to that of the gas–pyroclast jet of the First Cone of the Tolbachik 1975 eruption (gas is H_2O, $T \sim 1100$°C, $x = 0.05$), we obtain: $u_s^{\max} = 900$ m s^{-1}, $u_s^{\min} = 175$ m s^{-1}.

The pyroclasts are polydisperse, and some particles can be defined as 'small' and some as 'large'. If the mass fraction of small particles in the pyroclasts is designated as f_s, the approximate formula for the velocity of sound in a gas–pyroclast mixture can be written as:

$$u_s = \sqrt{\frac{p}{\rho_g\left(1+\frac{f_s}{x}\right)}} \approx \sqrt{\frac{xp}{f_s\rho_g}} \tag{52}$$

The zone boundaries with different flow structure are calculated from the volume relationships between phases. On the lower boundary of the bubbling flow zone (zone 2 in Fig. 2b) pressure is defined by Eq. 12 at $V_g = 0$, or by Eq. 2, substituting $c = c_0$. The upper boundary of the bubbling zone (the beginning of foam disruption) is defined by the gas volume fraction ($V_g/V_l \sim 3$). The boundary between zones of partly destroyed foam and gas–pyroclast dispersion volume fraction of free gas phase, δ_0, is defined with a value 0.44.

4.1.4. Numerical solution

The solution includes numerical integration of the differential equation of momentum, Eq. 33 along the conduit. Pressure was used as the vari-

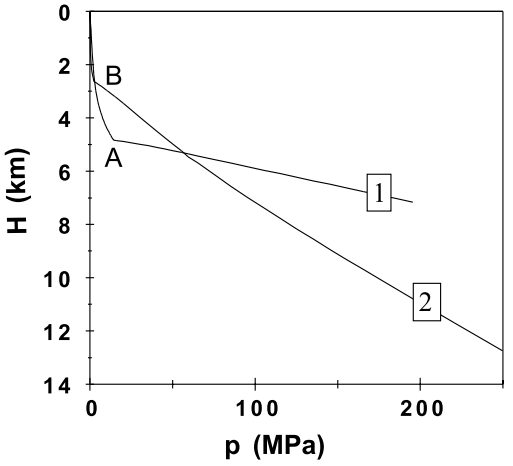

Fig. 6. Pressure variations with height along conduits of volcanoes with different types of magma. (1) Model of the Mount St. Helens 1980 eruption ($H=7.2$ km, $U\sim1$ m s^{-1}, $a=0.0060$ MPa$^{-1/2}$, $d_p=0.001$ m, $c=0.046$); (2) model of the First Cone at the Northern Breakthrough of the Tolbachik 1975 eruption ($H=25$ km, $U\sim0.1$ m s^{-1}, $a=0.0032$ MPa$^{-1/2}$, $d_p=0.01$ m, $c=0.05$). Points A and B indicate fragmentation levels for these eruptions.

able of integration, because all the characteristics of the flow depend on it and it is defined at both ends of the conduit. Geometrical and substantial parameters of the system and mass discharge rate of magma were fixed at the start of integration. Integration started at one end of the conduit with the corresponding boundary condition and proceeded to the other end. By varying magma mass discharge rate one can obtain the second boundary condition. Taking into account the boundary condition at the conduit exit, it is convenient to start integration from the upper end down, opposite to the direction of magma flow.

4.2. Quantitative characteristics of magma flow in a volcanic conduit

4.2.1. Pressure changes along the conduit

Calculated pressure changes along the conduit for two different eruptions are shown in Fig. 6. A silicic magma and shallow magma chamber (curve 1) approximately correspond to Mount St. Helens 1980. Basalt magma and a deep magma chamber approximately correspond to the First Cone at Northern Breakthrough at Tolbachik. In both cases p_{ex} (see Eq. 2) was assumed equal to +20 MPa at the start of the gas–pyroclastic eruption. These two examples differ in the relative and absolute length of the dispersion zone. For Mount St. Helens it is about 5 km and occupies much more than half of the conduit; in the Tolbachik case it is 2.6 km and occupies only $\approx$10% of the conduit length. In both cases the pressure in the conduit is less than the hydrostatic pressure of a magma column without bubbles (which is near to lithostatic). The pressure difference between magma in the conduit and the pressure in the surrounding rock is largest at the fragmentation level (points A and B in Fig. 6). It is about 105 MPa for Mount St. Helens and 60 MPa for Tolbachik. For such large pressure differences destruction of the conduit walls by a process similar to mining burst (Kravchenko, 1955) is probable. This destruction was indicated by lava bombs with xenolith cores at the Northern Breakthrough (Slobodskoy, 1977; Kovalev and Kutyev, 1977).

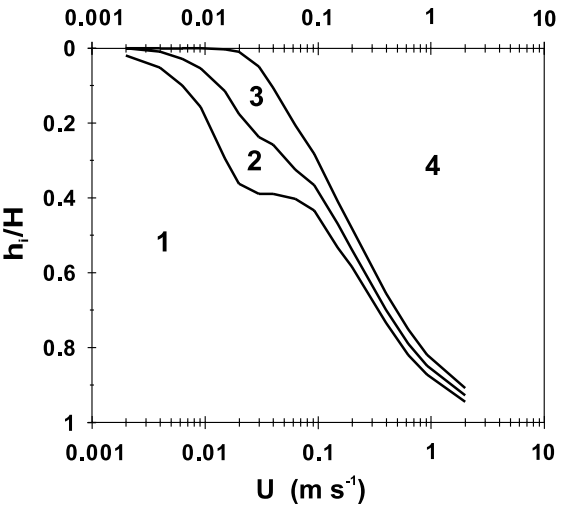

Fig. 7. Map of the relative lengths of the zones with different flow structures, h_i/H versus magma ascent velocity for the dispersion regime. Curves are the boundaries dividing the zones with different flow structures; h_i is the length of zone i. Zone 1 ($i=1$) is the homogeneous melt; zone 2 is the bubbling flow; zone 3 is the partly destroyed foam (PDF); zone 4 is the dispersion of a two-phase gas–pyroclastic mixture. Parameters used in the calculations: $c_0=0.046$; $a=0.0060$ MPa$^{-1/2}$; $\sigma=10^{-4}$ m^2/Pa s; $d_p=0.001$ m; $p_{ex}=0$.

Table 3
Values of the conduit conductivity (σ) and magma viscosity (η) calculated for two possible magma ascent velocities (U) and different possible water contents

U (m s^{-1})	c_0	σ (m^2 Pa^{-1} s^{-1})	η (Pa s) (b = 1.2 m)
0.10	0.05	0.00018	8×10^3
	0.07	0.00010	1.4×10^4
	0.09	0.00006	2.4×10^4
0.16	0.05	0.00024	6×10^3
	0.07	0.00014	1×10^4
	0.09	0.000075	1.9×10^4

4.2.2. Length of zones with different flow structures

The relative lengths of zones with different flow structure calculated for $p_{ex}=0$ and other parameters corresponding to the eruption of Mount St. Helens (except H and U) are shown in Fig. 7. At values of U of about 0.001 m s^{-1}, nearly the whole conduit is filled with the homogeneous melt; at $U\approx0.02$ m s^{-1}, the lengths of the bubble and PDF zones reach their maximum values of about 0.2 and 0.2, respectively, of the conduit length and the zone of dispersion flow appears; at $U>0.1$ m s^{-1}, the bubble and PDF zones become narrow and the dispersion zone enlarges dramatically.

4.2.3. Some estimates for the Tolbachik eruption

Field data from the Tolbachik eruption (Fedotov, 1984) allow calculation of magma viscosity in the conduit using the model and comparison with the measured viscosity of lavas. The width and the horizontal length of the fissure, the depth of the magma chamber, the mass discharge rate and the volatile content of the magma were estimated by direct measurements. A feasible range of magma ascent velocities (0.10–0.16 m s^{-1}) and water contents (0.05–0.09, assuming a phreatic origin for the latter value (Menyaylov et al., 1980)) were used. Values of $\sigma=b^2/\eta$ and viscosity η were then calculated (Table 3). The viscosity estimates range from one to one and a half orders of magnitude less than 3×10^5 Pa s, measured on the initial lava flow at the base of the First Cone (Fedotov, 1984; Vande-Kirkov, 1978)). Differences between calculated and measured viscosities are reasonable, as the basalt is expected to increase in viscosity due to degassing during ascent.

5. Controls of the magma mass discharge rate on dynamic stability and the nature of catastrophic explosive eruptions

5.1. Basic governing parameters

There are numerous parameters that influence a volcanic system, but not all of them are independent and their influences are not of equivalent value. Appropriate sets of the basic governing parameters need to be chosen. The influence of other important parameters can then be studied (see Section 5.4). In general, the magma mass discharge rate depends on the driving pressure, that is, on the difference between the values of the pressure at both ends of the conduit minus the hydrostatic pressure of the magma in the conduit, and on the total hydraulic resistance of the conduit. These characteristics depend on the conduit length, H, and the flow resistance in the region of liquid flow. Conduit resistance depends on its characteristic cross-dimension b and magma viscosity η, parameters which appear in the pertinent equations in a fixed combination (e.g. conduit conductivity defined as $\sigma=b^2/\eta$ in Eq. 4). The pressure difference between the conduit ends is

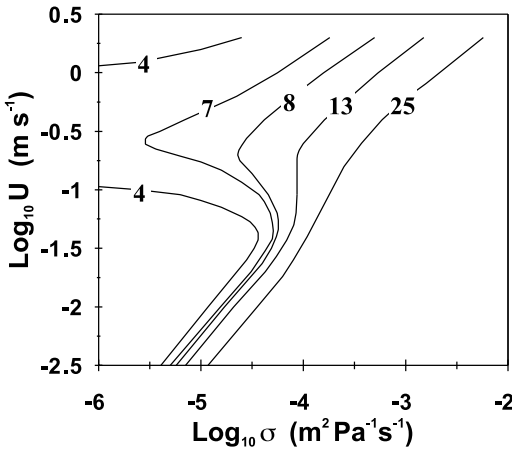

Fig. 8. Magma ascent velocity, U, plotted as a function of the conduit conductivity for different conduit lengths in kilometers. Figures near the curves represent values of the conduit lengths; other parameter values are: $c_0=0.05$; $a=0.0041$ MPa$^{-1/2}$; $\rho_l=2700$ kg/m^3; $\rho_{ga}=0.16$ kg/m^3; $d_p=0.01$ m; $\beta=0.3$; $p_{ex}=40$ MPa, and correspond to typical values for the Tolbachik eruption, 1975.

mostly dependent on magma chamber pressure. However, it is more convenient to use excess pressure p_{ex}, (Eq. 2) as a governing parameter. Both p_{ex} and the driving pressure difference have positive values just before the beginning of an eruption and later p_{ex} monotonically decreases to negative values, but driving pressure can change up and down, in some cases dramatically. It is useful to consider the influence of two parameters with the third fixed. Let us fix p_{ex} first and consider the dependence of magma mass discharge rate on conduit length and conductivity.

5.2. *Magma mass discharge rate as a function of the length and conductivity of the conduit*

Sets of curves expressing the magma ascent velocity, U, as a function of conduit conductivity were calculated at different values of chamber depth (Fig. 8). Here magma ascent velocity is proportional to magma discharge rate. Two types of curves are found: (1) every value of σ corresponds to a single value of U (curves for $H > 13$ km in Fig. 8); (2) every value of σ corresponds to three values of U (curves for $H < 13$ km in Fig. 8). These two types of curves are separated by some critical conduit length H_{cr}, which equals 13 km in the models in Fig. 8. If magma ascent velocity as a function of two variables (H and σ) is put on a three-dimensional graph, a curved plane (equilibrium surface) is obtained with a singularity of cusp type (Fig. 9), which describes the standard 'catastrophe' of two-parameter families of functions (Poston and Stewart, 1978; Arnold, 1979;

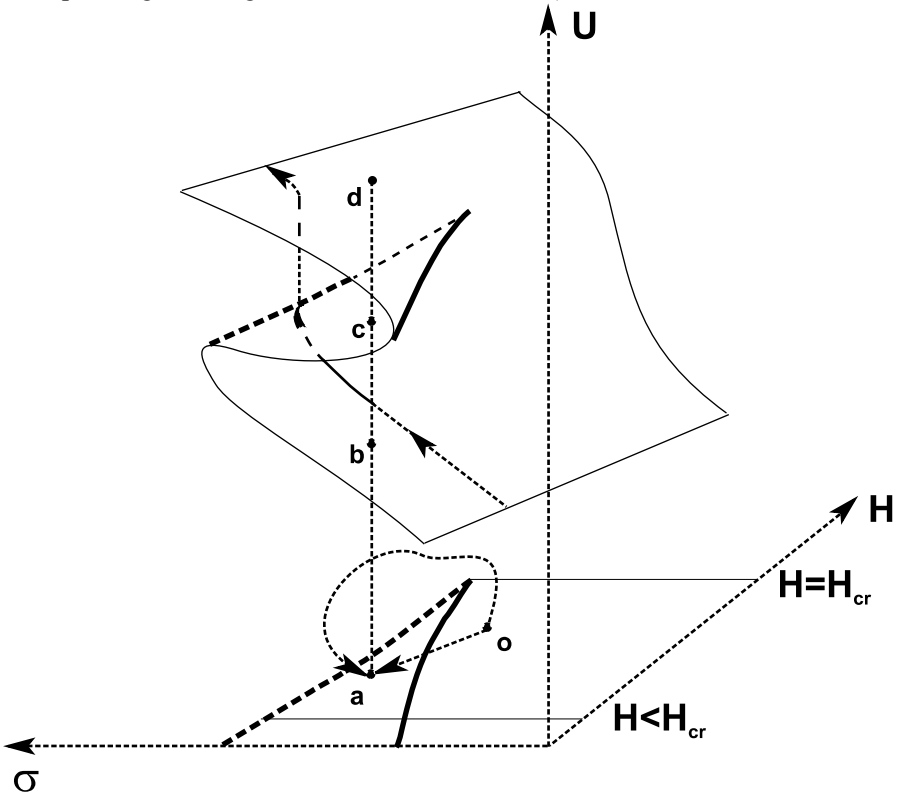

Fig. 9. Magma ascent velocity as a function of governing parameters H and σ. The curved plane is an equilibrium surface of the standard catastrophe of two-parameter function with cusp-like singularity (two folds converging onto a cusp). It is drawn as an illustration without calculated figures on the axis. Point 'a' in the σ–H plane has three images in the equilibrium surface ('b', 'c' and 'd') showing three feasible states of an eruption. The line with arrows on the equilibrium surface is the trajectory of the image point showing changes due to the conductivity increase at the beginning of an eruption with a sharp increase of the eruption intensity. Two lines connecting points 'o' and 'a' on the σ–H plane indicate two possible smooth evolution paths leading to different points ('b' and 'd') on the equilibrium surface.

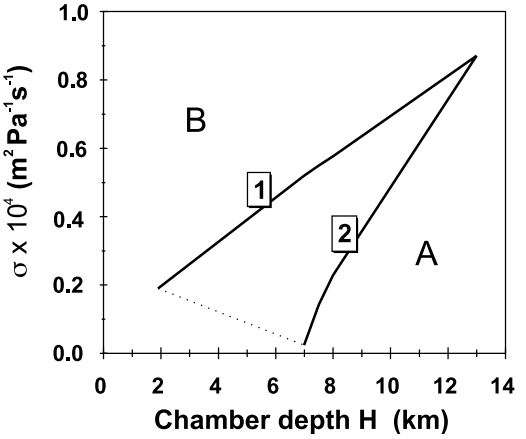

Fig. 10. Projection of the 'cusp' on the plane of the governing parameters (chamber depth and conduit conductivity) or map of catastrophe. Calculated using the same parameters as for Fig. 8. Inside the angle, between lines 1 and 2, every point corresponds to three values of magma velocity: two stable regimes with low and high intensity ('lower' and 'upper' regimes) and one unstable intermediate intensity regime. Region A corresponds to the 'lower' regime only; region B, to the 'upper' (much more intensive) regime.

Gilmore, 1981). Every point on the equilibrium surface indicates a steady state and changing of the steady states can be described by moving such an indicative (or image) point over this surface. 'Catastrophe' here indicates a sharp, dramatic change of the state of a system caused by the small and smooth change of a governing parameter. In the case of a volcano this mathematical term coincides with the practical (common) meaning of catastrophe.

Projection of the singularity on the plane of the two governing parameters or the 'map of the catastrophe' is shown separately (Fig. 10). It has the form of an angle made by two lines connected to the cusp, which are projections of the folds of the equilibrium surface and represent the 'separatrix of the catastrophe'. Every point on the plane inside this angle has three images on the equilibrium surface, and outside only one. If the image point on the plane passes across the separatrix, the function (magma ascent velocity) can undergo an abrupt change or 'catastrophe'. Such an 'evolutionary track' is shown in Fig. 9. As a 'standard catastrophe' of two-parameter families of functions a cusp singularity has structural stability in that is it is not changed as a qualitative feature if all the parameters are changed by some small but finite amount. This indicates some standard stable behavior of an erupting volcano.

In Fig. 11 a vertical section of the equilibrium surface is shown. It has three branches (limbs), and three points of intersection of any vertical line with these branches reflect three different regimes corresponding to one value of conductivity. The upper and lower branches describe stable regimes, whereas the middle branch (between A and C in Fig. 11) describes an unstable regime. If the point describing the state of the system is on the lower branch of the graph, and the conductivity of the conduit gradually increases, at the reversal of the curve at A the conditions must jump to the upper branch (from point A to point B in Fig. 11). The magma velocity, and therefore the mass discharge rate, increases by an order of magnitude. In some cases the increase can be up to three orders of magnitude and more. If the conditions move to the left on the upper branch (conductivity decreases), it must eventually jump to the lower branch (from C to D) and magma mass discharge rate decreases abruptly. This decrease could be from one order of magnitude to infinity, when the eruption stops entirely.

The set of curves in Fig. 8 corresponds to the start of the eruption (p_{ex} maximum). The decrease

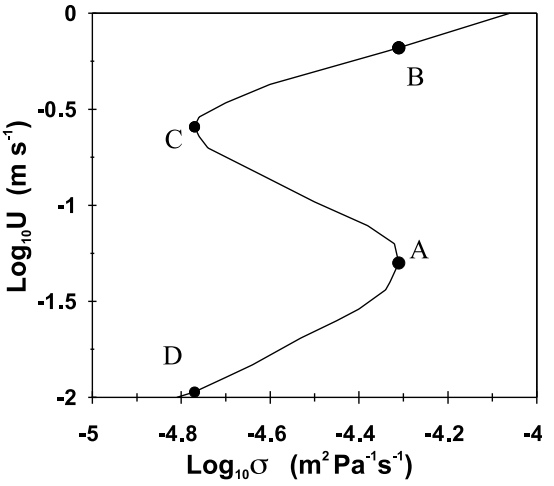

Fig. 11. Magma ascent velocity as a function of conductivity of the conduit in the region of the 'cusp' (qualitative picture). The points A, B, C and D are discussed in the text.

of pressure does not change the qualitative picture, but moves the whole set of curves to the side of higher conductivities and stretches the region of multiple states in the horizontal direction.

A governing parameter is called *splitting* if any change moves the image point through the cusp point in the direction of the cusp axis. A change of splitting parameter along the cusp axis leads to *bifurcation* of the process at the cusp point. Behind it there are two possible paths for the point: the system can progress along either the upper or lower limb (sheet) of the folded equilibrium surface (Fig. 9). The value of the splitting parameter defines the feasibility of two values of U (low and high) and of abrupt changes between them. A parameter which drives the point indicating the state of the system perpendicular to the cusp axis is called *normal*. The moment of abrupt change of U depends on its value. In the volcanic case none of the chosen governing parameters can be called splitting, but the conduit length is closest. Conduit length changes very little during eruptions, although conduit length can vary between volcanoes. Conduit conductivity is a normal parameter, which varies greatly during an eruption and determines conditions for abrupt change if $H < H_{cr}$ at constant p_{ex}. The critical conduit length H_{cr} corresponds to the point of the cusp.

If conductivity increases from a small value and the indicative point moves from region A to reach line 1 (Fig. 10), a jump to the upper part of the folded plane occurs (magma discharge rate increases abruptly). The physical mechanism of this jump is as follows. An increase of magma discharge rate results in two effects: (1) increase of magma ascent velocity and a corresponding increase in the resisting friction forces; (2) increase of the region of gaseous flow with a corresponding decrease of the liquid flow region and average magma density in the conduit, resulting in a decrease of the total flow resistance and an increase of the driving pressure difference. If the absolute length of the liquid flow region is small enough (as it is when $H < H_{cr}$) the second effect prevails with positive feedback. As a result, magma mass discharge rate increases dramatically up to the state when total resistivity in the liquid flow region becomes less than that in the gaseous flow region (the length of the liquid flow region should be much less than 1% of the total for this) or the critical flow velocity at the exit is reached (the choking condition).

These principles show how an eruption can abruptly change states between explosive and effusive activity. Using three principal governing parameters the influence of other parameters on the evolution of an eruption can be studied.

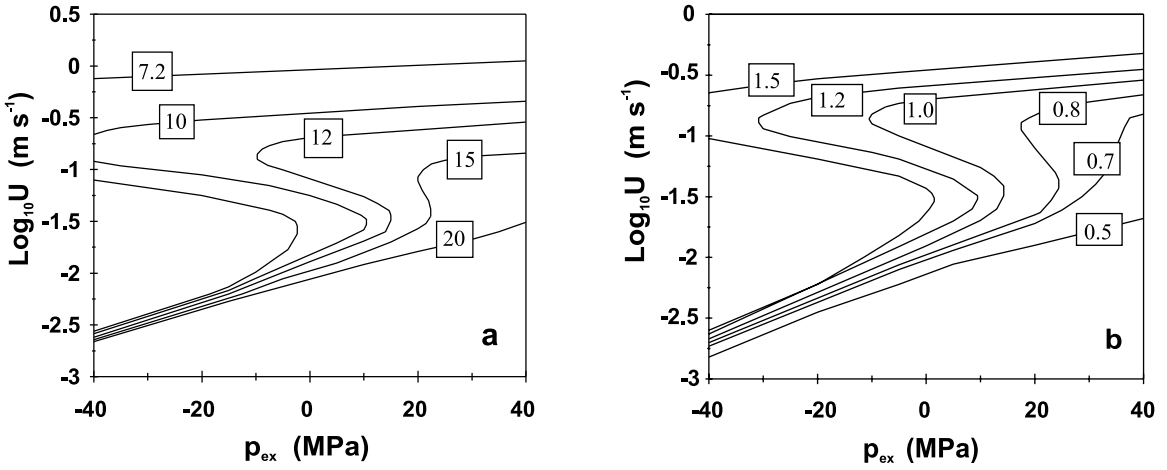

Fig. 12. The dependence of magma ascent velocity on the excess pressure p_{ex}. (a) Conduit conductivity $\sigma = 10^{-4}$ m^2 Pa^{-1} s^{-1} is fixed. Numbers on the curves are chamber depth in km. (b) Chamber depth $H = 12$ km is fixed. Numbers on the curves are conductivity of the conduit in 10^{-4} m^2 Pa^{-1} s^{-1}.

5.3. Magma mass discharge rate as a function of chamber pressure

The dependence of the magma discharge rate on any other pair of governing parameters including p_{ex} has the same form of cusp catastrophe. p_{ex} is a normal parameter. In Fig. 12 such dependencies are calculated for an eruption similar to that of Mount St. Helens 1980 with volatile fraction 0.046, average particle size 0.001 m, average particle porosity 0.3, melt density 2500 kg m^{-3}, gas density 0.2 kg m^{-3} at atmospheric pressure and magma temperature, and coefficient $a = 0.0060$ $MPa^{-1/2}$. In Fig. 12a the conductivity of the conduit is fixed and the chamber depth is varied, and vice versa in Fig. 12b. These two figures illustrate the similarity of the influence of conduit length and conductivity on magma ascent velocity. When the region of liquid flow is large enough, a several-fold change of H has nearly the same effect as a change of σ in the same proportion. However, when the relative length of the liquid flow zone is small, a change of H is more effective than a change of conductivity (compare Fig. 12a with Fig. 12b).

5.3.1. Change of the position of the cusp point

Magma discharge rate changes are described by the indicative (image) point movement over the *equilibrium surface* of the catastrophe. Instability and discharge rate jumps can appear when the indicative point intersects the line of a fold on the equilibrium surface. Such an intersection can occur either as a result of the indicative point moving or the cusp singularity moving. The position of the cusp singularity (Fig. 9) depends on the coordinates of the cusp point (H_{cr} and σ_{cr}), which depend on the value of p_{ex} and other magma system properties. Both critical values increase significantly when p_{ex} decreases (Fig. 13). The increase of H_{cr} leads to an increase of the feasibility of mass discharge rate jumps: at a value of p_{ex} a little under zero a discharge rate jump becomes feasible at any magma chamber depth. The increase of the critical conduit conductivity, in contrast, decreases the feasibility of a discharge rate jump. Such opposite tendencies do not exclude the theoretical possibility of jump-like increases of magma discharge rate due to decrease of p_{ex} when the magma chamber is situated at rather large depths. But in this case implausibly large increases of conductivity of the conduit at depth are needed near the end of eruption.

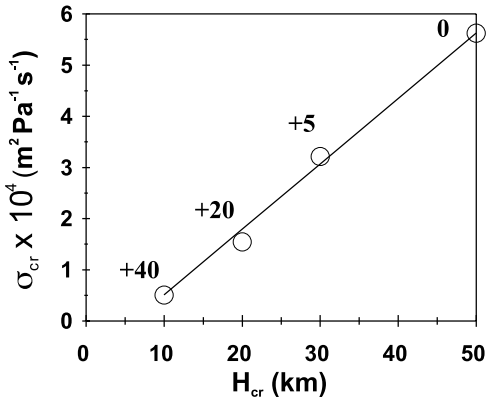

Fig. 13. Change of the position of the cusp point on the coordinate plane $H_{cr}-\sigma_{cr}$ as a result of a p_{ex} change calculated for the parameters corresponding to the Tolbachik eruption (see Fig. 8 for values). The value of p_{ex} in MPa is shown near the points on the graph.

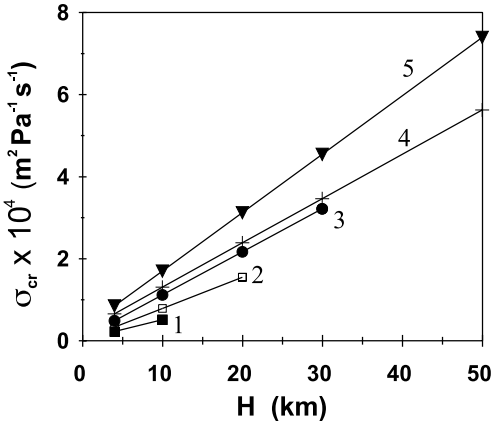

Fig. 14. The dependence $\sigma_{cr}(H)$ at $H < H_{cr}$ calculated at different values of p_{ex}. (1) $p_{ex} = 40$ MPa ($H_{cr} = 10$ km), (2) $p_{ex} = 20$ MPa ($H_{cr} = 20$ km), (3) $p_{ex} = 5$ MPa ($H_{cr} = 30$ km), (4) $p_{ex} = 0$ ($H_{cr} = 50$ km), (5) $p_{ex} = -5$ MPa ($H_{cr} \gg 50$ km).

5.3.2. Change of the cusp boundaries

When $H < H_{cr}$, the function $\sigma_{cr}(H)$ is represented by the upper boundary line of a cusp at which a jump up can occur (the axis line of the

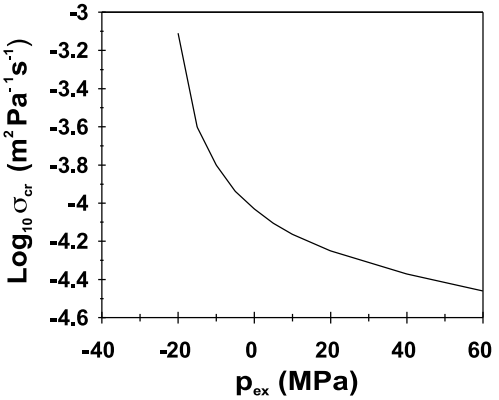

Fig. 15. The dependence $\sigma_{cr}(p_{ex})$ calculated for Mount St. Helens ($H=7.2$ km, $a=0.0060$ MPa$^{-1/2}$, $c=0.046$).

lower fold in Fig. 9, line 1 in Fig. 10), and is a straight line. Sets of such straight lines are shown in Fig. 14, calculated for different values of p_{ex}. The function $\sigma_{cr}(p_{ex})$, calculated for Mount St Helens ($H=7.2$ km), is shown in Fig. 15. There is a very steep increase of σ_{cr} when p_{ex} becomes less than zero. The greater the chamber depth or the less the excess pressure, the larger the value of conduit conductivity required for the jump to the upper (catastrophic) regime. These conditions are contradictory: naturally, conduit conductivity tends to decrease if chamber depth increases or excess pressure decreases. This places limits on the chamber depth at which catastrophic jumps of eruption intensity can occur.

The lower boundary of the cusp (Fig. 10) is the projection of the axis of the upper fold (Fig. 9). When the indicative point on the projection intersects this line, its origin on the equilibrium surface falls from the upper to the lower limb of the folded surface and magma ascent velocity decreases abruptly. The critical conductivity at this jump is designated as $\sigma\downarrow$. The position of the boundary line changes slightly when chamber pressure decreases (Fig. 16). At small chamber depths all the lines converge and intersect at $\sigma\downarrow=0$ with H approximately equal to 7 km. The physical meaning of this intersection point is that at these (and lower) chamber depths the jump to the lower (extrusive) regime cannot occur at any σ up to 0. The upper regime should cease only after total evacuation of the chamber or destruction of the chamber roof or conduit walls. Such an eruption would not have an extrusion (PDF) stage (if the model assumptions are not changed).

The dependence $\sigma\downarrow(p_{ex})$ is a straight line on a semi-logarithmic scale at a constant chamber depth (Fig. 17). When the conduit conductivity is less than 1.5×10^{-5} m^2 Pa^{-1} s^{-1} a jump-like decrease of the magma discharge rate should take place at $p_{ex}=+60$ MPa, that is, the upper high-intensity regime is improbable. When the conduit conductivity is more than 2.5×10^{-5} m^2 Pa^{-1} s^{-1} the transition to the lower regime can take place only if p_{ex} falls to -40 MPa or less.

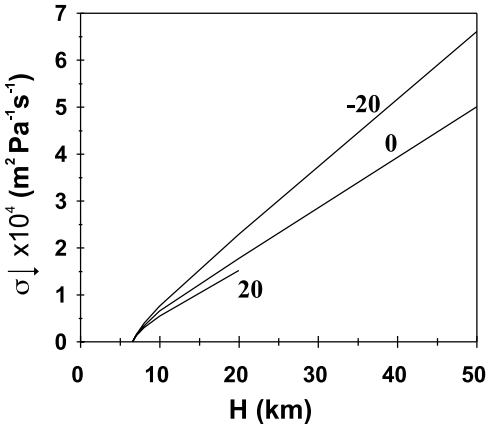

Fig. 16. The dependence $\sigma\downarrow(H)$ calculated for a volcano with parameters of Mount St. Helens (see Fig. 15) and different values of p_{ex}, which are written near the curves in MPa.

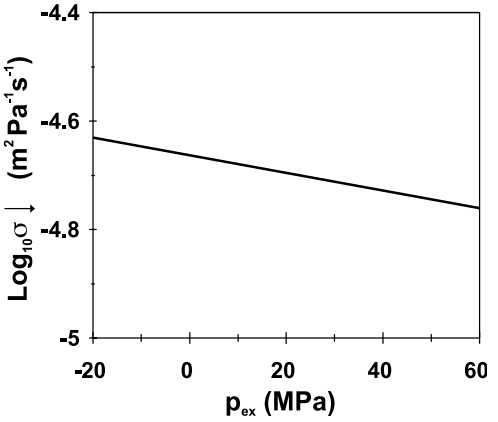

Fig. 17. Log($\sigma\downarrow$) as a function of excess pressure p_{ex} calculated for the Mount St. Helens volcano ($H=7.2$ km).

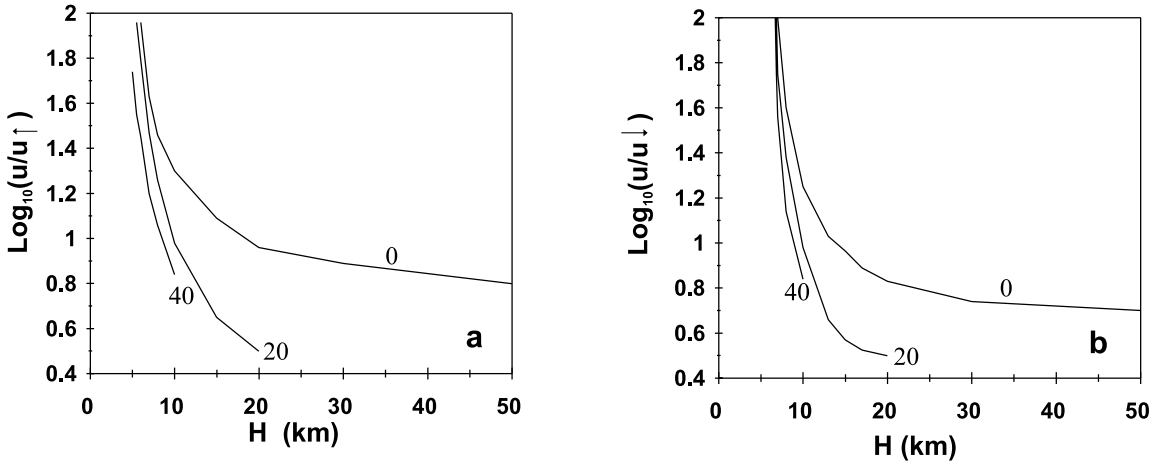

Fig. 18. Relative amplitude of the magma mass rate jump as a function of magma chamber depth calculated for a volcano similar to Mount St. Helens and the different excess pressures, which are indicated at the curves in MPa. (a) $u/u\uparrow$ (jump upward). (b) $u/u\downarrow$ (jump downward).

When the negative pressure becomes so large, the destruction of conduit walls and chamber roof becomes very likely, causing the regime change. Suitable values of σ lie in a narrow interval. This fact can be used for indirect estimates of conduit dimensions and magma properties.

For shallow magma chambers and volatile-rich magmas the fragmentation level can migrate down into the magma chamber. As the horizontal cross-sectional area of the chamber is several orders of magnitude larger than that of the conduit, the velocity of gas upflow in the magma chamber is not sufficient for fluidization of the pyroclast particles and so ejection of the condensed material must stop. Consequent subsidence of the pyroclasts and foam in the chamber can cause an eruption to stop and the chamber roof to collapse because of the lack of support. This mechanism of stopping an eruption should occur in most caldera-forming eruptions. Further considerations of magma discharge rate variations in large magnitude explosive eruptions can be found in Slezin and Melnik (1994) and Melnik (2000).

5.3.3. *Amplitude of the magma mass discharge rate jump on the cusp boundaries*

The amplitude of the discharge rate jump is defined as the absolute value of the ratio of the magma mass flux magnitudes before and after the jump and is denoted as $u/u\uparrow$ and $u/u\downarrow$. This ratio increases when chamber depth decreases with respect to critical depth and when p_{ex} decreases. Near H_{cr}, when H diminishes, the jump amplitude immediately reaches a factor of a few and then rises slowly at first but accelerates thereafter. The value of $u/u\uparrow$ increases close to exponentially and for shallow chambers can reach more than three orders of magnitude. The value of $u/u\downarrow$ increases

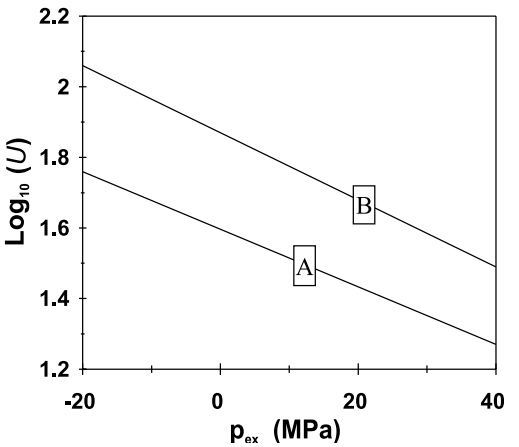

Fig. 19. Amplitude of the magma mass rate jump (U) as a function of p_{ex} calculated for a volcano similar to Mount St. Helens ($H = 7.2$ km). Here U is the change in velocity at the jump. Line A, $U = u/u\uparrow$ (jump upward); line B, $U = u/u\downarrow$ (jump downward).

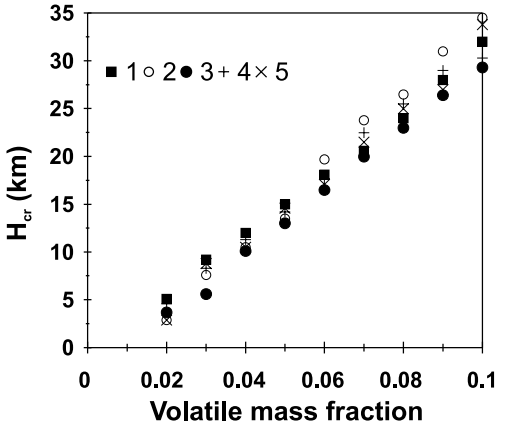

Fig. 20. Value of H_{cr} as a function of volatile (water) content in magma c_0 at $p_{ex}=20$ MPa. For other parameters the following values were used: (1) $d_p=0.001$ m, $\beta=0.75$, $a=0.0041$ MPa$^{-1/2}$; (2) $d_p=0.01$ m, $\beta=0.75$, $a=0.0032$ MPa$^{-1/2}$; (3) $d_p=0.0001$ m, $\beta=0$, $a=0.0041$ MPa$^{-1/2}$; (4) $d_p=0.001$ m, $\beta=0.3$, $a=0.0064$ MPa$^{-1/2}$; (5) $d_p=0.01$ m, $\beta=0.75$, $a=0.0041$ MPa$^{-1/2}$.

much faster and becomes infinite at the value of H at which the eruption stops entirely. Results of some calculations made for a volcano similar to Mount St. Helens are illustrated in Figs. 18 and 19.

5.4. The dependence of magma mass discharge rate on the magma properties

The dependence of cusp point coordinates H_{cr} and σ_{cr} on magma properties is now investigated (Slezin, 1994). Calculations of H_{cr} and σ_{cr} using a range of typical values of the volatile content c_0, solubility coefficient a, size of pyroclast particles d_p and their porosity β are shown in Figs. 20 and 21. For a fixed chamber pressure, H_{cr} depends predominantly on the volatile content c_0. The effect of the other parameters is relatively small and irregular (Fig. 20). All the points plot in a narrow zone close to a straight line, described by the equation:

$$H_{cr}(\mathrm{km}) = H^*(c_0 - c^*) \tag{53}$$

where $H^*=356$ km and $c^*=0.01$. The characteristic value $c_0=0.01$, at which H_{cr} became 0, approximately corresponds to the no-dispersion zone. An increase of c_0 leads to an increase of H_{cr} and H_{cr}/H and so increases the probability and amplitude of the sharp, jump-like increase of magma discharge rate. The limiting chamber depth at which instability and mass discharge rate jumps are possible is obtained by substituting $H=H_{cr}$ into Eq. 53. For $c_0=0.06$ as a maximum value, the limiting value of $H\sim 18$ km is calculated.

The value of σ_{cr} strongly depends on the size and porosity of particles and less strongly on the volatile content (Fig. 21). σ_{cr} decreases and the probability of magma discharge rate jump increases when volatile content and porosity of the particles increase and the particle size decreases. All the listed changes lead to an increase of particle velocity in the flow and consequently to a decrease of the flow density and an increase of the driving pressure difference.

5.5. Nature of catastrophic explosive eruptions

5.5.1. Types of catastrophic explosive eruptions and stages of their development

In catastrophic explosive eruptions (CEE) large masses of pyroclastic material are ejected in a short interval of time. Historic examples include Tambora (1815), Krakatau (1883), Bezymyanny (1956) and Mount St. Helens (1980) and prehistoric examples include Santorini, Greece (3400 BP) and Toba, Sumatra ($\sim$74 000 BP). In all these events the volume of erupted material greatly exceeded 1 km^3 and in the Toba eruption was more than 2000 km^3 (Gushchenko, 1979; Simkin and Siebert, 1994). The main and sometimes the only substage of a large CEE is a steady-jet stage. There can be flow unsteadiness due to external factors, such as collapse of conduit walls or chamber roof, and hydrodynamical pulsations. In this definition the steady-jet stage produces both pyroclastic fallout and pyroclastic flows, as they are generated by the same conduit flow structure. Pyroclastic flows can result from collapse of a vertical gas–ash column (Wilson, 1976; Sparks et al., 1978) fed by a steady conduit flow.

In some cases the steady-jet stage is preceded by a 'directed blast' (another substage of the catastrophic stage), which is usually caused by defor-

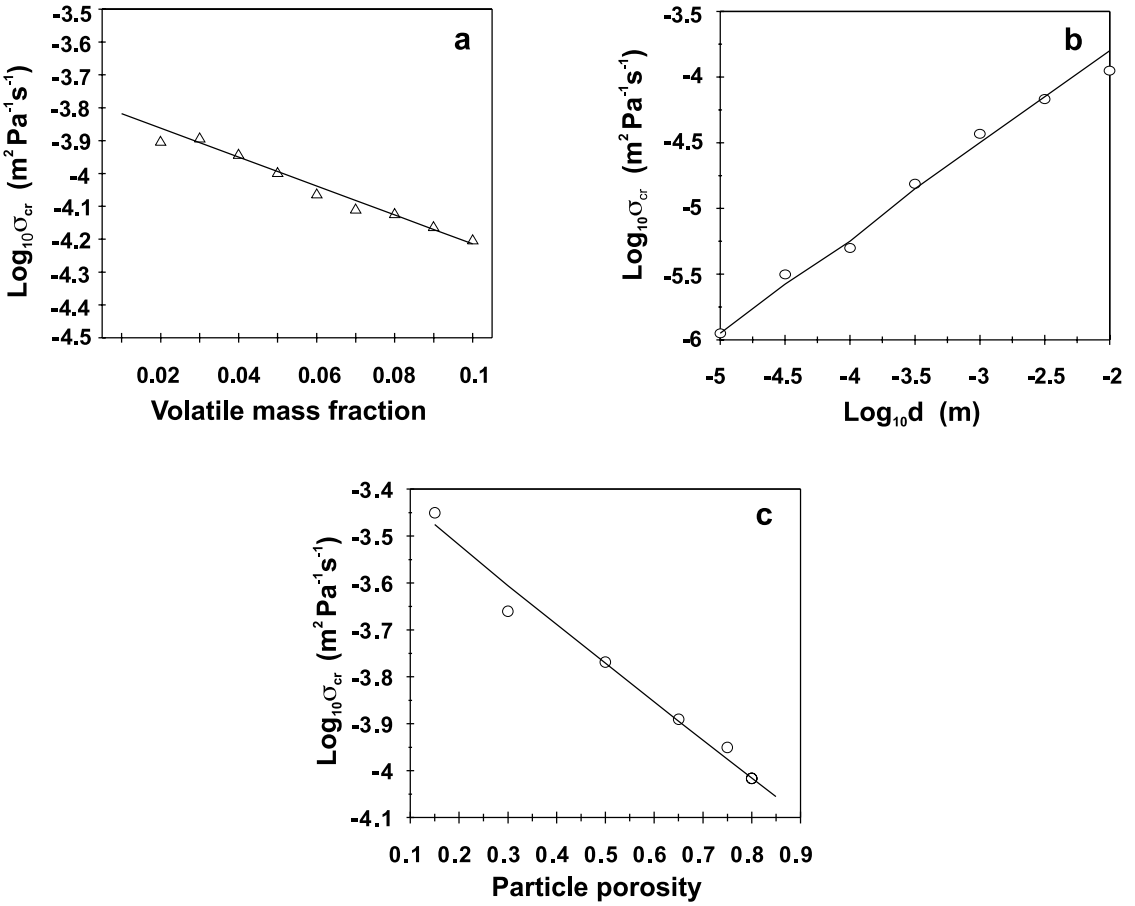

Fig. 21. Critical conductivity of volcanic conduit σ_{cr} as a function of different parameters. (a) The volatile (water) content. (b) The size of pyroclastic particles. (c) The particle porosity. In a, $p_{ex}=20$ MPa, $d=0.01$ m, porosity = 0.75. In b, $p_{ex}=20$ MPa, volatile content = 0.05, porosity = 0.75. In c, $p_{ex}=20$ MPa, volatile content = 0.05, $d=0.01$ m.

mation of a volcanic edifice and landslide. A directed blast partly destroys the volcanic edifice and ejects much old material. The catastrophic stage is sometimes preceded by a period of moderate activity, which could last from hours and days to several years and can provide significant amounts of juvenile pyroclastic products (Krakatau 1883 – 3 months, Bezymyanny 1956 – 5 months, Tambora 1815 – 3 years; (Gushchenko, 1979)). After the catastrophic stage in most cases an extrusive stage develops. After the end of or during the catastrophic stage of the largest of the CEE, caldera subsidence takes place. The start and end of the steady-jet stage occur abruptly with a sharp increase or decrease of the magma discharge rate by more than an order of magnitude (typically 2–3 orders and sometimes more).

5.5.2. *Mechanism of transition of eruption into catastrophic stage*

The theory described here can explain the principal features of CEE and their relationship to the characteristics of the magmatic system. The transition of an eruption into a catastrophic stage is described as an abrupt jump-like increase of the magma mass discharge rate, which takes place when conduit conductivity reaches its critical value. It can take place when the conduit length H is less than H_{cr}. This mechanism inevitably implies moderate activity preceding the catastrophic

stage. When an eruption starts, the upper part of the conduit is newly created. Magma intrudes into the new fissure in relatively cold rock and resistance to the magma flow is initially large. The image point of the system is expected to be on the lower branch (limb) of the curve in Fig. 11. As an eruption proceeds, the active flow of degassing magma erodes fissure walls and the magma heats the walls. These processes cause an increase in the cross-dimension of the conduit and a decrease of heat loss through the walls and so a decrease in magma viscosity. These processes increase conduit conductivity and so lead to an abrupt transition to an intensive regime related to the upper limb of the curve in Fig. 11. The amplitude of the mass discharge rate jump depends on the relationship between critical and actual length of the conduit H_{cr}/H. The greater this ratio, the greater is the amplitude of the jump (Fig. 22). The intense gas–pyroclast flow can enlarge the cross-sectional area of the upper part of the conduit, making a nozzle that allows supersonic flow. In the latter case the amplitude of the mass discharge rate jump can be up to several-fold larger.

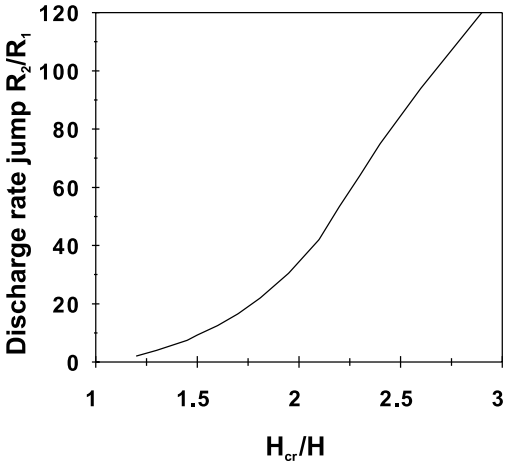

Fig. 22. Amplitude of the jump-like increase of magma mass flux at the beginning of the catastrophic stage of eruption as a function of the relation H_{cr}/H. R_1 and R_2 are the mass fluxes before and after the jump. The value of the critical conduit length H_{cr} was taken as 15 km. Other parameters except H are corresponding to the eruption of Mount St. Helens 1980. The possible development of a supersonic nozzle is not taken into account.

Magma chamber depths are reliably known for only a few volcanoes where CEEs have taken place. However, all available data suggest that depths are shallow. Geophysical studies have located magma chambers under young calderas at depths of 5–6 km (Yokoyama, 1969; Zubin et al., 1971; Gorshkov, 1973; Zlobin and Fedorchenko, 1982; Sanders, 1984; Ferrucci et al., 1992; Smith and Braile, 1994; Miller and Smith, 1999). Calculated critical values of magma chamber depths for the corresponding volcanoes are about 15 km (three times larger than the estimated depths). These high values of H_{cr}/H correspond to mass discharge rate jump amplitudes of more than two orders of magnitude and the onset of very intensive steady-jet regimes.

A directed blast is a natural 'trigger' for the steady-jet stage, because destroying the upper part of the volcanic edifice shortens and widens the conduit. A sector collapse also can act as the trigger of a steady-jet stage, but it is more effective as a trigger of a directed blast.

5.5.3. *Final stage of the catastrophic explosive eruption*

The catastrophic steady-jet stage stops abruptly (Gorshkov and Bogoyavlenskaya, 1965; Williams and Self, 1983; Fedotov, 1984). In some cases, an extrusive stage follows with a magma mass discharge rate about three orders of magnitude less than that during the catastrophic stage. In other cases the eruption stops entirely. The theory related here predicts this behavior and suggests that an abrupt stop to a CEE corresponds to the shallowest magma chambers.

5.6. *General description of the evolution of eruption in a steady-state approximation*

The steady-state approximation describes eruption evolution as a succession of steady states for changes that are very slow. Also, the transient period of a new steady state is considerably shorter than the time of the system's existence in a new state. Though changing of eruption regime from moderate to catastrophic can be nearly instantaneous, the formation of the new stable flow structure in the conduit can take considerable time.

Slezin (1997) estimated a time of approximately 3 h for the eruption of Mount St. Helens, three times less than the duration of the steady-jet stage. For similar eruptions, transient times of a catastrophic stage must be of the same order. The transient time from a catastrophic to an extrusive stage can be considered as the time interval between the end of the steady-jet stage and the appearance of the extrusive dome.

5.6.1. Evolution of the dispersion regime

The evolution of an eruption involves three governing parameters: conduit conductivity, conduit length and the excess chamber pressure. The magma discharge rate as a function of any two of these parameters can be expressed by the equilibrium surface with a standard cusp catastrophe. The function of all three parameters is a combination of the several cusp catastrophes and is a three-dimensional plane in a four-dimensional space. The corresponding catastrophe separatrix is two-dimensional surface in a space of three dimensions. Projections of the cusp singularities on the p_{ex}–σ plane calculated for the different H are shown in Fig. 23. On the three-dimensional graph with chamber depth as a third coordinate a three-dimensional image of the separatrix of the catastrophe resembles the edge of a cutter. In practice, the dimensions of this cutter-like separatrix should be limited by the real values of parameters in volcanic systems.

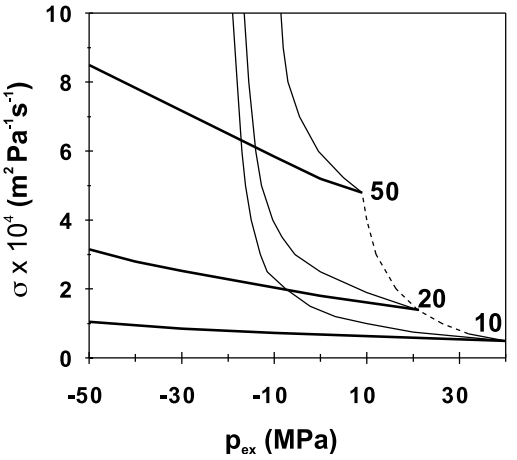

Fig. 23. Maps of catastrophe on the plane p_{ex}–σ calculated for a volcano similar to Mount St. Helens and different chamber depths. Bold lines are the lines of the folds describing the jump-like decrease of magma mass rate; thin lines correspond to the folds describing the jump-like increase of magma mass rate. Figures near the cusps (the point where the two lines intersect) are the values of the magma chamber depth in km. The dashed line shows the location of this intersection (cusp) point in p_{ex}–σ space.

Available data suggest that maximum magma chamber depths should be about 50 km. When $H = 20$ km, instability and jumps of magma mass flow rate are possible only if $\sigma > 0.00015$ m^2 Pa^{-1} s^{-1}, and when $H = 50$ km, only if $\sigma > 0.0005$ m^2 Pa^{-1} s^{-1} (Fig. 23). The likelihood of the first value is very small and the second value is practically impossible. So the maximum chamber depth for which catastrophic increases of magma mass discharge rate occur must be no more than approximately 20 km. Direct observations of volcanic conduits at depth are not possible, but the theory discussed here can be used to estimate conduit conductivity. Using parameters for Mount St. Helens in 1980 (see Section 3.4.2), the sharp decline in discharge rate at the end of the steady-jet stage could take place only if the conductivity was in the range $(2–3)\times10^{-4}$ m^2 Pa^{-1} s^{-1}. The initial excess pressure is controlled by the strength of the overlying rock and by hydrostatics. The minimum excess pressure at the end of eruption depends on the strength of the walls of the conduit and the chamber roof. The maximum pressure is limited by the *long-lived* strength of *material*; the minimum pressure is limited by the *instantaneous* strength of the roof as a *structure*. To estimate the latter value is much more difficult than the former. The minimum value of p_{ex} is assumed to be about −100 MPa, and in most cases it is no more than −40 to −50 MPa.

In the evolution of an eruption, a change of the governing parameters involves a continuous and monotonic decrease of the chamber pressure. Initially, the conduit conductivity is expected to increase and in the final stage to decrease, due to the decrease of magma upward velocity and so the increase of relative heat and volatile losses. Conduit length usually has a constant value. However, in intensive eruptions the erupted products are widely dispersed, the supersonic jet can produce a shallow crater, and thus the length of

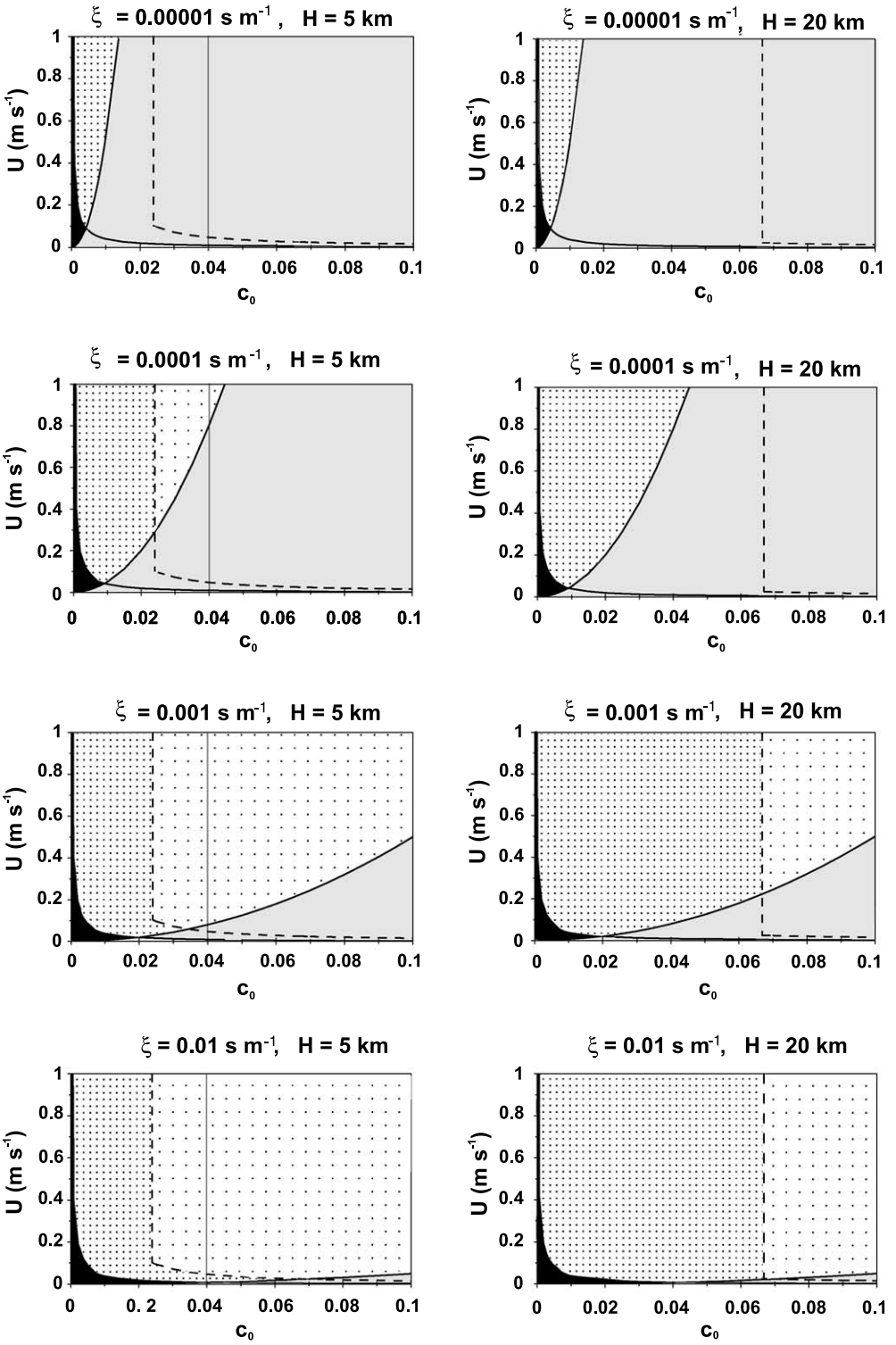
ξ = 0.00001 s m-1, H = 5 km
ξ = 0.00001 s m-1, H = 20 km
ξ = 0.0001 s m-1, H = 5 km
ξ = 0.0001 s m-1, H = 20 km
ξ = 0.001 s m-1, H = 5 km
ξ = 0.001 s m-1, H = 20 km
ξ = 0.01 s m-1, H = 5 km
ξ = 0.01 s m-1, H = 20 km
U (m s-1)
c0
0
0.2
0.4
0.6
0.8
1
0.02
0.04
0.06
0.08
0.1

the conduit decreases. The prehistoric eruption of Taupo, New Zealand in AD 180 is an example (Walker, 1980; Wilson and Walker, 1985).

Besides these standard smooth changes of governing parameters there are other kinds of variations. The conduit can be shortened by destruction of the volcanic edifice by landslide or explosion. The conduit and chamber roof may be destroyed by subsidence. New deeper magma can enter the chamber. The model can predict the qualitative effects of such processes through their influences on the main governing parameters. All these additional factors add complications, but do not affect underlying principles.

The following 'standard' scenarios for the evolution of an eruption are described:

(1) $H > H_{cr}$. Magma mass discharge rate increases monotonically; then, after a smooth wide maximum, the rate decreases also monotonically but rather sharply. At the end of the eruption an extrusion could appear.

(2) $H < H_{cr}$. *Magma chamber is small and relatively deep*. Magma mass discharge rate increases and then decreases monotonically, being small at all stages of eruption.

(3) $H < H_{cr}$. *Magma chamber is not very deep and of rather large volume*. Magma mass discharge rate increases monotonically, then sharply increases by several orders of magnitude, changing to an explosive steady-jet stage, and finally decreases sharply to an extrusive stage.

(4) $H < H_{cr}$. *Rather small and very shallow magma chamber*. A scenario similar to that described in (3), but with a more rapid increase of intensity at the start and the eruption completely stopping after steady-jet stage (extrusive stage is absent).

(5) $H < H_{cr}$. *Shallow and rather large magma chamber*. Scenario is the same as in (3) and (4), but with caldera subsidence at the end of eruption. At the end of subsidence extrusion is possible.

5.6.2. Map of the basic eruption regimes

To describe the general evolution of a volcanic eruption the region of the catastrophic conditions is added to a map of the three basic regimes (see Fig. 4). The boundaries of the catastrophic region can be found specifically only by means of numerical calculations, but for general analysis simplified analytic expressions can be obtained from numerical calculations.

The value of U before a jump-like increase is $u\uparrow$. It decreases as volatile content increases. For example, $u\uparrow$ equals 0.025 m s^{-1} at $c = 0.06$ to about 0.1 m s^{-1} at $c = 0.02$. $u\uparrow$ can be approximately derived by equating the driving pressure difference to the pressure loss due to friction over the conduit length. After some transformations the expression for $u\uparrow$ is (Slezin, 1997):

$$u\uparrow = \frac{\sigma\uparrow}{H} F(c, d_p, p_{ex}) \tag{54}$$

The function $F(c, d_p, p_{ex})$ is weakly dependent on its arguments and to a first approximation can be considered to be a constant, the value of which is obtained by numerical calculations.

The value of $\sigma\uparrow$ (σ_{cr}) is linearly dependent on H (Fig. 14). If H/H_{cr} replaces H on the abscissa in Fig. 14 all the inclined lines on the graph have the same length and would differ only by the angle of inclination to the horizontal axis, which increases as p_{ex}decreases. All the lines intersect the abscissa at a point a little to the left of the origin. Thus:

$$\sigma\uparrow = A(p_{ex})\frac{H}{H_{cr}} + B(p_{ex}) \tag{55}$$

Fig. 24. 'Maps of regimes' of eruptions for the different types of magma and chamber depths. Black area gives the region of the extrusive regime; grey area gives the region of the DGS regime; densely dotted area gives the region of the moderate dispersion regime; lightly dotted area gives the region of the transition to the catastrophic dispersion regime. The descending line on each graph describes $U_d(c)$ given by Eq. 31, that is, the upper boundary of the extrusive regime; the ascending line describes $U_{cr}(c,\xi)$ given by Eq. 21, that is, the upper boundary of the DGS regime; the descending dashed line with the vertical section is the lower boundary of the region where the catastrophic jump of magma mass discharge rate takes place. Its vertical straight section corresponds to Inequality 59, and the hyperbolic curve section corresponds to Eq. 57. On all graphs the hyperbolic part of the last curve was calculated at $p_{ex} = 20$ MPa, corresponding to the initial stage of eruption. Thin vertical lines on the four left graphs are examples of an evolution path of eruption.

For a magma system similar to that of Mount St. Helens the value of $A(p_{ex})$ is approximately 20 times that of $B(p_{ex})$ and to a first approximation $B(p_{ex})$ can be neglected. When $p_{ex} > 0$ and the jump-like increase of magma mass discharge rate is feasible, $A(p_{ex})$ can be described as

$$A(p_{ex}) = \frac{a}{b + p_{ex}} \tag{56}$$

where $a = 0.0033$, $b = 35.5$ MPa and p_{ex} is in MPa. Substituting Eq. 56 and H_{cr} from Eq. 53 into Eq. 55, putting $B(p_{ex}) = 0$, and then substituting Eq. 55 into Eq. 54, one finally obtains:

$$u\uparrow = \frac{A}{(b + p_{ex})(c_0 - c^*)} \tag{57}$$

Numerical calculations give for the case of Mount St. Helens $A = 0.08$. The value of $u\uparrow$ is independent of H.

To determine boundaries of the catastrophic conditions on the regimes map, condition 58 should be taken into account:

$$H < H_{cr} \tag{58}$$

As H is fixed and H_{cr} is variable the combination of condition 58 with Eq. 53 gives the inequality:

$$c_0 > H/H^* + c^* \tag{59}$$

The limit value of c_0:

$$c_0^{\min} = H/H^* + c^* \tag{60}$$

also gives the boundary of the region for magma discharge rate jumps and can be added to Eq. 57.

All possible eruption states are determined in the map coordinates by relations 21, 31, 57 and 60. Variants of maps are shown in Fig. 24 for an initial $p_{ex} = 20$ MPa. The descending hyperbolic line on each graph describes the relation $U_d(c)$ given by Eq. 31, indicating the upper boundary of the extrusive regime; the ascending line describes the relation $U_{cr}(c,\xi)$ given by Eq. 21, indicating the upper boundary of the DGS regime; the descending line, Eq. 57, with the vertical section, described by Eq. 60, is the lower boundary of the region where a catastrophic jump of magma discharge rate takes place. The dispersion regime can occur at the parameter values lying in the region above both of these two curves. A change to the catastrophic regime can take place above all three curves (and to the right of the vertical part of the last curve).

Illustrative evolutionary paths of an eruption in Fig. 24 follow a vertical line at constant c_0 starting near the abscissa at $U = 0$ and with velocity increasing with time. The regime changes if a boundary line is crossed. Consider, for example, $H = 5$ km and $c_0 = 0.04$ (Fig. 24). In the first (top) graph ($\xi = 10^{-5}$ s m^{-1}, corresponding to basalts) the whole path is in the region of the DGS flow; in the second graph ($\xi = 10^{-4}$ s m^{-1}) a change to the catastrophic explosive regime (CEE) from the DGS regime is feasible, but requires a high velocity of magma ascent; in the third graph ($\xi = 10^{-3}$ s m^{-1}) most of the path occurs in the region of the catastrophic jump, which occurs directly from the DGS regime; on the last, bottom, graph ($\xi = 10^{-2}$ s m^{-1}, corresponding to rhyolites) the DGS regime and the extrusive regime both occur for very small magma ascent velocities, then these regimes change to the moderate steady-jet regime and then to CEE. If the catastrophic regime is possible it should start from a DGS regime. A moderate steady-jet regime between these two can take place in a rather small interval of c_0 values and small U values at large values of ξ.

Direct transition from the extrusive to the catastrophic regime as a result of smooth evolution requires very large values of ξ and very small magma ascent velocities. This transition can be triggered by other processes. Destruction of an extrusive dome and volcanic edifice with a subsequent explosion can trigger a CEE, as took place in the eruption of Mount St. Helens in 1980.

Condition 60 limits the region of catastrophic jumps to small chamber depths. At a magma chamber depth of 20 km a catastrophic jump is possible only if the volatile content exceeds 6.6 wt% (Fig. 24). If water contents are typically less than 6.6%, then 20 km is an upper limit on the magma chamber depth at which the catastrophic regime can occur. In Section 5.5.1 the same value of about 20 km for the maximum

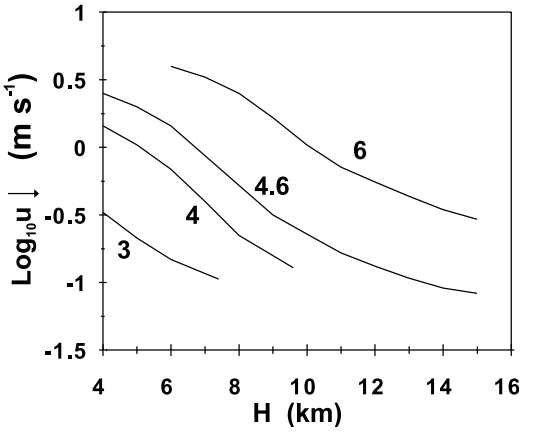

Fig. 25. Dependence of the velocity of magma ascent just at the moment of cessation of the steady-jet stage of eruption ($u\downarrow$) on magma chamber depth at the different values of volatile (water) content. The velocity here refers to the value just before the jump down to a lower velocity. Figures near the curves are volatile (water) content in wt%. Curves are calculated at $\sigma = 10^{-4}$ m^2 Pa^{-1} s^{-1} and at the values of the other parameters, except H, approximately corresponding to eruption of Mount St. Helens, 1980.

chamber depth was obtained by other considerations.

All the graphs in Fig. 24 describe conditions at the beginning of an eruption and help to describe the evolution of the eruption before a catastrophic jump and at the moment of the jump. The amplitude of the jump cannot be deduced from these graphs. To describe evolution after a transition to the steady-jet regime these graphs should be supplemented to show the amplitude of magma mass discharge rate jumps before and after the steady-jet stage. A decrease of the magma mass discharge rate will not follow the same path as its increase. The abrupt changes from the steady-jet to the PDF regime or to a complete cessation occur at much higher discharge rates than the changes from the DGS to a steady-jet regime. The final stages of an eruption can be described by another map. In Fig. 25 the velocity of the eruption is shown at the moment just before the cessation of the steady-jet regime and the following decrease to a much lower velocity regime. Curves are shown for different water contents as a function of chamber depth.

6. Some effects connected with eruption

6.1. Evacuation of magma chamber

This section develops a model of a magma chamber evacuation during explosive eruptions causing caldera formation based on the analysis of Slezin (1987) published in Russian. This work complements studies by Druitt and Sparks (1984), Lipman (1984) and Roche et al. (2000).

6.1.1. Theoretical description

The cause of caldera subsidence due to an explosive eruption is evacuation of a magma chamber, which weakens the support of the chamber roof and results in a pressure decrease, with exsolution of gas in the chamber. To a first approximation the deficit of magma volume in the chamber is equal to the total gas volume in it. Subsidence of the roof finally stops when the pressure needed for its support is restored. Subsidence takes place when all foaming magma has left the chamber or the conduit becomes blocked. In the last case the residual gas in bubbles would dissolve back into the magma as the pressure is restored.

Magma chamber evacuation is characterized by the value of 'magma drawdown' $\Delta = V/A$ (Smith, 1979; Spera and Crisp, 1981), where V is the erupted volume reduced to dense magma and A is the area of the caldera, assumed to be equal to the area of horizontal projection of the magma chamber. Expressing V through erupted mass M and magma density ρ_l, one can obtain:

$$\Delta = \frac{M}{\rho_l A} \tag{61}$$

The problem is to find Δ as a function of the characteristics of the magma system.

The magnitude of draw-down must depend strongly on the relation in time between processes of chamber evacuation and roof subsidence. If the eruption continues during subsidence, nearly total evacuation of the chamber is possible, and the magma draw-down Δ would be approximately equal to the mean vertical dimension of the chamber. If the eruption stopped before the beginning of subsidence, the value of Δ would depend on the

eruption dynamics and the flow structure in the conduit. Geological data suggest that both alternatives exist. Lipman (1986) demonstrated that simultaneous eruption and collapse occur in caldera-forming eruptions (10^2–10^3 km^3). In smaller-magnitude eruptions subsidence begins after the eruption has stopped. In some eruptions evacuation of the magma chamber was not accompanied by caldera subsidence at all.

Evacuation of a chamber begins when the level of bubble nucleation reaches chamber depths and stops when magma movement through the conduit becomes impossible. This approximation results from the model assumptions of an incompressible condensed component of magma and a rigid chamber. Evacuation of the magma chamber can stop in one of the following three cases: (1) when the excess pressure is not sufficient to move magma through the conduit; (2) when the conduit is blocked; (3) when the fragmentation level is in the chamber. In the last case outflow of pyroclast particles stops because in a chamber (where the cross-sectional area is much larger than in a conduit) upward velocity of gas is not sufficient to suspend particles. When the fragmentation level reaches the magma chamber, support of the chamber roof will have decreased dramatically and its collapse becomes inevitable. So, it follows that the eruption stops when the volume fraction of gas bubbles at the roof of the chamber, β_0, corresponds to the limit of the foam stability. This volume fraction is expected to be near to the state of close packing equal to 0.74.

The value of pressure and the volume fraction of the gaseous phase at the lower end of a conduit is obtained by numerical solution of Eqs. 32–36. In a chamber these values can be obtained by a static approximation. The vertical coordinate is denoted z and is directed downward, with the origin at the roof of the magma chamber. At $z=0$, $p=p_0$ and $\beta=\beta_0$; at $z=z_1$ the pressure $p=p_1$ at which the gaseous phase disappears: $\beta_1=0$. The volatile content c_0 is assumed to be constant throughout the magma chamber with solubility dependent only on pressure (Eq. 2).

In the static one-dimensional case the following expression for magma draw-down can be written:

$$\Delta = z_l - \frac{p_1 - p_0}{g\rho_l} \tag{62}$$

To evaluate p_0, p_1 and z_1, first the dependence of β on the pressure should be found. Per unit mass of magma this can be written as:

$$\beta = \frac{V_g}{V_g + V_l} \tag{63}$$

For the static problem, and neglecting surface tension effects, we can write:

$$V_g = \frac{c_0 - c}{\rho_g} \tag{64}$$

$$V_l = \frac{1-(c_0 - c)}{\rho_l} \tag{65}$$

Substituting Eqs. 65 and 64 into Eq. 63 and taking into account dependencies of the solubility and density of gas on pressure, we obtain:

$$\beta = \frac{1}{1 + Bp\dfrac{1-(c_0-c)}{c_0-c}} \tag{66}$$

where $B=\rho_{ga}/(p_a\rho_l)$.

The typical values of (c_0-c) are of order 10^{-2}, so Eq. 66 can be simplified to:

$$\beta = \frac{1}{1 + \dfrac{Bp}{c_0-c}} \tag{67}$$

From Eq. 67 the values of the pressure corresponding to the upper (p_0) and lower (p_1) boundaries of the zone with decreased magma density can be obtained (substituting β_0 or 0 correspondingly instead of β):

$$p_0 = \frac{1}{4}\frac{a^2}{B^2}\left(\frac{1-\beta_0}{\beta_0}\right)^2\left(\sqrt{1+\frac{4Bc_0\beta_0}{a^2(1-\beta_0)}}-1\right)^2 \tag{68a}$$

$$p_1 = \frac{c_0^2}{a^2} \tag{68b}$$

Density depends on porosity β in the following way:

$$\rho = \rho_g\beta + \rho_l(1-\beta) \tag{69}$$

Substituting Eq. 67 and expressions for c and ρ as a function of p into Eq. 69, after simple transformations the following expression for ρ can be obtained:

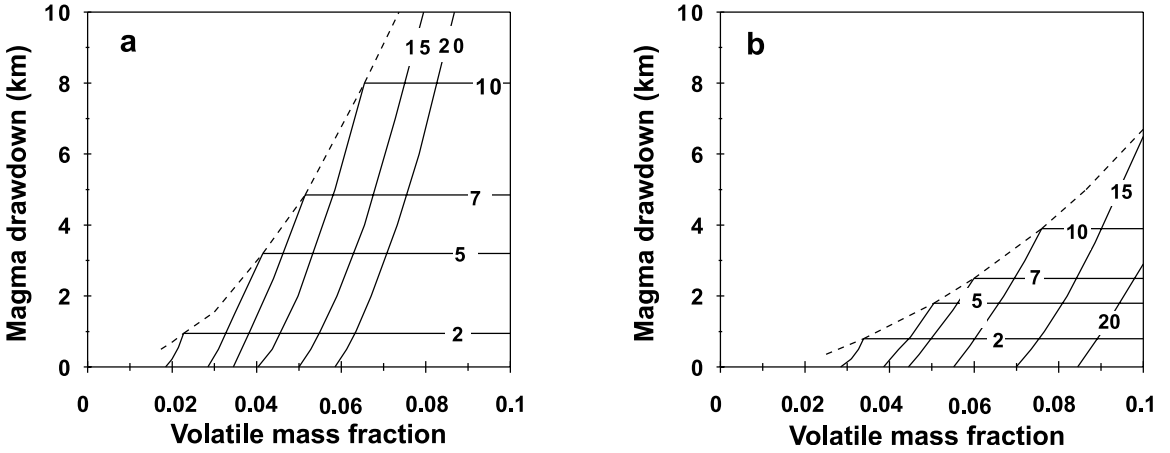

Fig. 26. The dependence of magma draw-down on the volatile (water) content calculated for the different depths of magma chamber. The curves are marked for the depth of the magma chamber in km. (a) Solubility coefficient $a = 0.0041$ MPa$^{-1/2}$. (b) Solubility coefficient $a = 0.0064$ MPa$^{-1/2}$.

$$\rho = \rho_l \frac{Bp(c_0 - a\sqrt{p} + 1)}{c_0 - a\sqrt{p} + Bp} \tag{70}$$

The depth where the first bubbles appeared can be calculated as the integral:

$$z_1 = \int_{p_0}^{p_1} \frac{dp}{g\rho} \tag{71}$$

where ρ is determined by Eq. 70. After some transformations one obtains:

$$z_1 = \frac{1}{Bg\rho_l}\left[\frac{c_0}{c_0+1}\ln\frac{p_1}{p_0} + 2\left(\frac{1}{(c_0+)B} - \frac{c_0+1}{a^2}\right)\right.$$

$$\left.\ln\frac{c_0 - a\sqrt{p_1} + 1}{c_0 - a\sqrt{p_0} + 1} - \frac{2}{a}(\sqrt{p_1} - \sqrt{p_0})\right] \tag{72}$$

Eq. 72 can be simplified a little if expanded in series logarithms using the small parameter $c_0 - a\sqrt{p}$ and leaving only the first members of the series:

$$z_1 = \frac{1}{Bg\rho_l}\frac{c_0}{c_0+1}$$

$$\left[\ln\frac{p_1}{p_0} + 2\left(\frac{(c_0+1)B}{a} - \frac{a}{c_0}\right)(\sqrt{p_1} - \sqrt{p_0})\right] \tag{73}$$

Substituting Eqs. 68 and 73 into Eq. 62, the dependence of the magma draw-down on the initial volatile content in the magma c_0, the solubility coefficient a, the gas density at atmospheric pressure ρ_{ga} and the maximum porosity at the chamber roof β_0 is obtained.

6.1.2. Results of calculations

Maximum magma draw-downs for the different combinations of parameters are shown in Fig. 26. Every curve starts at some minimum volatile content, which increases as the chamber depth increases and solubility coefficient, a, increases. For typical water contents the maximum chamber depth at which partial evacuation is possible is about 15 km when $a = 0.0041$ MPa$^{-1/2}$ and about 10 km when $a = 0.0064$ MPa$^{-1/2}$. At greater depths slight evacuation is only likely if the water content exceeds 5%. Every curve has a break at the water content corresponding to the fragmentation level reaching the top of the chamber. After this break the curve transforms into a straight line parallel to the abscissa. A curve drawn through the break-points describes some optimum combination of the volatile content and the depth of the magma chamber roof for effective evacuation. It shows a minimum value of volatile (water) content at which the maximum value of Δ corresponding to a fixed value of H can be reached. If the volatile content is more than this optimum the additional gas has no influence on magma draw-down for a fixed chamber depth, because after destruction of the foam in the chamber the

outflow ceased. The range of c in which the magnitude of magma draw-down Δ changes from zero to its maximum value is about 0.01. These dependencies put definite limits on the values of H, c, and Δ. The increase of Δ is possible due to increase of H only if at the same time the minimum and optimum values of c also increase.

6.1.3. Comparison with observations

Water content is typically estimated between 0.04 and 0.06 for the most catastrophic eruptions. Magma chamber roof depths estimated by various geophysical methods are between 5 and 7 km (Balesta, 1981; Zlobin and Fedorchenko, 1982; Walker, 1984; Denlinger and Riley, 1984). The maximum magma draw-down for such parameters of the magma system is calculated as about 3 km. Approximately the same value of 3 km was found as a maximum draw-down by Spera and Crisp (1981) from observational data. For the Mount St. Helens eruption (18 May 1980) $c = 0.046$, $H = 7.2$ km, magma chamber diameter $D_{ch} \sim 1.5$ km, $V = 0.25$ km^3 (Sarna-Wojcicki et al., 1981; Rutherford et al., 1985). Using these data, draw-down is calculated as $\Delta \sim 0.12$ km. All these characteristics correlate well for $a \sim 0.0060$ MPa$^{-1/2}$, a typical value for rhyolitic melts (Fig. 26).

6.2. Variations of intensity and pauses in the dispersion regime of eruption

Significant variations of magma mass discharge rate and relatively short-lived periods of inactivity can take place during the dispersion regime. The largest instability of the flow regime and pauses occur near critical points of eruption before the sharp changes. On the First Cone of the Tolbachik eruption 1975–1976, numerous pauses with durations of minutes to a few hours (with subsequent restoring of flow intensity) preceded the appearance of lava flows at the South of the First Cone and the start of the Second Cone eruption.

New magma boccas, which developed near the active cone in the Tolbachik eruption, are thought to be connected to new magmatic fissures branching from the main conduit. Every new lava breakthrough was preceded by shallow volcanic earthquakes due to propagation of new fissures (Fedotov, 1984). A new fissure requires magma outflow from the main conduit. Thus magma mass discharge rate in the main conduit is decreased and is then gradually restored before the next impulse. The change of magma mass discharge rate influences the flow structure and eruption regime. Decrease of the magma mass discharge rate causes a decrease of the dispersion zone length, and the average density of magma in the conduit increases. The density increase requires additional magma, so at the conduit exit the discharge rate decreases much more than at depth, which can cause a pause. The new average density and additional magma mass required for it can be calculated. The maximum possible duration of the pause can be calculated as a relation of the additional mass in the conduit to the magma mass discharge rate in the new flow state.

This maximum duration can be achieved in the case of instantaneous reaction of the flow at the step-like mass discharge rate change. The actual flow reaction is not instantaneous. A gradual decrease of magma mass discharge rate before the pause and an increase after it would shorten the pause. If the time of mass discharge rate restoration is less than the characteristic time of flow response on disturbance, a pause would not take

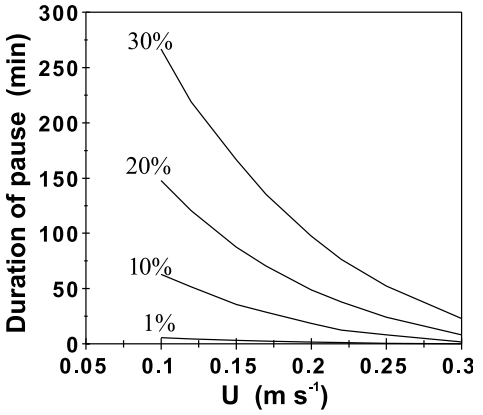

Fig. 27. Maximum duration of the pause in a steady-jet gas–pyroclastic eruption as a function of the magma ascent velocity. Figures on the curves are the values of the step-like percentage decrease of magma mass discharge rate.

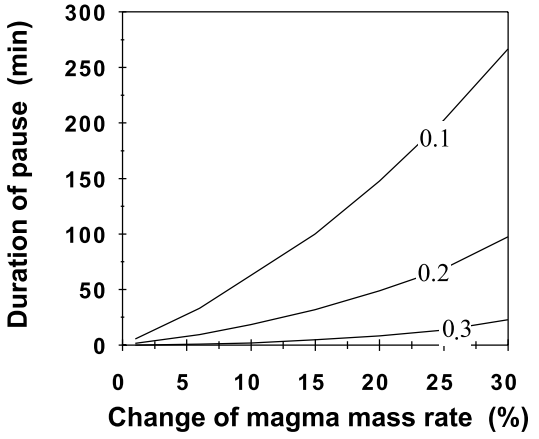

Fig. 28. Maximum duration of the pause in a steady-jet gas–pyroclastic eruption as a function of the values of the step-like percentage decrease of magma mass discharge rate. Figures on the curves are the magma ascent velocities (m s^{-1}).

place at all. The characteristic time of the flow response on disturbance, t_r, is the sum of the time needed for the disturbance to propagate through the conduit to the vent, t_c, and the time of relaxation of the particle velocity after decrease of the velocity of gas, t_{rel}. For the Tolbachik eruption the time of flow response to an instantaneous change of magma mass flux at the fragmentation level is estimated as 30 s (Slezin, 1982b). It is not a large time and so the proposed cause of a pause seems reasonable.

Flow response in the vent to the partial outflow at depth depends on the location of the outflow. Outflow at the entrance to the conduit is equivalent to enlargement of its cross section and increase of the total magma mass discharge rate from the chamber, but magma mass discharge rate through the conduit above the outflow level remains unchanged. If outflow takes place near the fragmentation level there is little influence on the total magma mass discharge rate from the chamber, because the total resistance of a conduit depends on the conditions in the region of liquid flow below the fragmentation level. So the magma mass discharge rate above the level of outflow would be less by the value of outflow, which affects the flow density and magma mass discharge rate at the exit. The generation of the new fissures during the Tolbachik eruption and accompanying seismic events suggests that outflow was not far below the fragmentation level. The possible maximum duration of pauses t_{max} was estimated, supposing that the outflow took place just below the fragmentation level. Calculations of t_{max} for the First Cone of the Tolbachik eruption are shown in Figs. 27 and 28.

The relative length of the zone of gas–pyroclast flow and the average magma density in a volcanic conduit strongly depend on the volatile content and on the effective diameter of particles. A sharp change of these parameters could take place if magma composition were changed, for example from a stratified magma chamber (Spera and Crisp, 1981). Calculations confirm that under ideal conditions, when the compositional change and flow response are nearly instantaneous, there should be pauses of the same duration as in the case of flow diversion at depth (Slezin, 1982b). However, in this case the flow response time is not so small as in the case of diversion. The disturbance propagates with the velocity of the flow and so a complete pause is unlikely.

6.3. Problem of prediction of volcanic eruptions

Prediction is crucial in the mitigation of eruptions. There are two principal issues: (1) prediction of when the eruption starts; (2) prediction of the characteristics of the eruption. The second part includes prediction of magnitude, intensity and violence of eruption and prediction of the duration of eruption and changes of regime. The theory describes the dependence of an eruption on the characteristics of the magma system and so can constrain the characteristics of future eruptions. The theory makes this task easier because it defines a small number of principal parameters of the magma system and provides criteria for predicting catastrophic changes of intensity.

7. Concluding remarks

Volcanic eruptions are treated as a quasi-steady process of magma outflow from a chamber through a narrow vertical conduit. Magma is considered as a two-component two-phase medium.

'Quasi-steady' means that changes of the flow parameters very little disturb the equilibrium between phases: equilibrium is restored much faster than the parameters change. Such an approach is usual in volcanological models, which vary in assumptions and methods of analysis. This theory was developed in Russia and was not known in the west, where analogous but not identical results were obtained independently and later.

The type of eruption depends on the two-phase flow structure at the exit of the conduit. This structure depends on many characteristics of the magma system, including its geometry, the magma properties and the dynamical characteristics of the process. Three principal types of magma flow structure and consequently three principal types of eruption are proposed: (1) discrete gas separation (DGS) regime – bubble flow; (2) dispersion regime – gas–pyroclast suspension flow; (3) regime of partly destroyed foam (PDF) – porous permeable flow. Criteria for the occurrence of each regime have been obtained, and depend on several parameters: magma ascent velocity; magma viscosity; number of bubble nuclei per unit volume of magma; volatile content; volatile solubility; and particle size and cohesive forces between particles.

The analysis of the dispersion regime demonstrates multi-state conditions and flow instability leading to an abrupt transition to another steady-state flow regime, changing magma discharge rate by several orders of magnitude. The principal characteristic of magma flow in a volcanic conduit that makes it unstable is the great difference in flow resistance between the regions with liquid viscous flow and gas-suspension flow, which can differ by 6–10 orders of magnitude. Steady-state theory cannot describe jump-like changes in detail, but it can characterize steady regimes before and after the jump, and define the conditions needed for the change of regimes. For the latter purpose the right choice of basic governing parameters incorporating all other parameters is necessary and these are identified as magma chamber depth, conduit conductivity and excess chamber pressure.

As a function of the basic governing parameters, magma discharge rate is described as a combination of cusp catastrophes. The main splitting parameter, which defines the position of the cusp point and the possibility of a catastrophe, is in most cases magma chamber depth. Normal parameters are conduit conductivity and chamber pressure. Magma discharge rate as a function of governing parameters creates an equilibrium surface. A point on this surface describes the state of the erupting volcano. Movement of this point over the surface describes changes in the state when governing parameters change. Intersections of the fold lines on this surface indicate sharp changes of the system state to a new stable regime, which can be predicted using the steady-state approach.

The jumps of magma discharge rate, described by the steady-state theory, are the mechanism of catastrophic explosive eruptions, in which sharp increases of intensity ('explosions') usually take place after moderate activity. The principal requirement for an increase of intensity is relatively small depth of the magma chamber. So the theory can be used as a basis for the prognosis of the potential danger of a volcano. The steady-state theory can also be used for the analysis and prediction of many other sharp changes in eruption behavior induced by internal dynamics as well as by external factors. This was illustrated by examples of caldera subsidence and pauses in gas–pyroclast jets. Steady-state theory can describe the evolution of an eruption as a succession of steady states with sharp transitions between them.

Acknowledgements

This work was supported by the Russian Foundation for Basic Research. The visit to Bristol University to prepare this paper was supported by the Royal Society of London. The author is grateful to Steve Sparks for useful discussions and advice, which have helped to improve the paper and for his enormous work in correcting the English text. The author also thanks O. Melnik for help connected with computer processing. The author is grateful to Elisabeth A. Parfitt and Karl L. Mitchell for detailed reviews of the manuscript with many helpful comments.

References

Alidibirov, M.A., Kravchenko, N.M., 1988. Experimental study of fluidization of the material of the pyroclastic flows of the eruption of Bezymyanny volcano (in Russian). Vulkanol. Seismol. 2, 98–104.

Arnold, V.I., 1979. Catastrophe theory (in Russian). Priroda 10, 54–63.

Balesta, S.T., 1981. Earth Crust and Magmatic Chambers in the Regions of the Modern Volcanism. Nauka, Moscow, 133 pp. (in Russian).

Balyshev, S.O., Savelyeva, B.V., Medvedev, V.Ia., 1996. On the problem of the shock decompression of silicate rocks (in Russian). Dokl. AN RAN 347, 66–68.

Barmin, A.A., Melnik, O.E., 1990. Gas-rich magma flow in volcanic conduit (in Russian). Izv. AN SSSR Ser. MLG 5, 23–25.

Barmin, A., Melnik, O., Sparks, R.S.J., 2002. Periodic behaviour in lava dome eruptions. Earth Planet. Sci. Lett. 199, 173–184.

Belousov, A.B., Bogoyavlenskaya, G.E., 1988. Debris avalanche of the 1956 Bezymyanny eruption. In: Kagoshima Int. Conf. on Volcanoes, 1988. Abstracts, p. 352.

Blower, J.D., Keating, J.P., Mader, H.M., Phillips, J.C., 2001. Inferring volcanic degassing processes from vesicle size distributions. Geophys. Res. Lett. 28, 347–350.

Boothroyd, R., 1971. The Flow of Gas with Suspended Particles. Chapman and Hall, London, 289 pp.

Burnham, C.W., Davis, N.F., 1974. The role of H_2O in silicate melts, II: Thermodynamic and phase relations in the system $NaAlSi_3O_8$-H_2O to 10 kbars, 700° to 1100°C. Am. J. Sci. 274, 902–940.

Carey, S., Sigurdsson, H., Gardner, J.E., Criswell, W., 1990. Variations in column height and magma discharge rate during May 18, 1980 eruption of Mount St. Helens. J. Volcanol. Geotherm. Res. 43, 99–112.

Chugaev, R.R., 1975. Hydraulics. Energia, Leningrad, 600 pp. (in Russian).

Clark, S.P., Jr. (Ed.), 1966. Handbook of Physical Constants. Revised edn. Yale University, New Haven, CT. Geol. Soc. Am. Memoir 97, 587 pp.

Crisp, J.A., 1984. Rates of magma emplacement and volcanic output. J. Volcanol. Geotherm. Res. 20, 177–212.

Deich, M.E., Philippov, G.A., 1968. Gas-dynamics of the Two-phase Media. Energia, Moscow, 423 pp. (in Russian).

Denlinger, R.P., Riley, F., 1984. Deformation of Long Valley Caldera, Mono County, California, from 1975 to 1982. J. Geophys. Res. 89, 8303–8314.

Dingwell, D.B., Bagdassarov, G., Bussod, G., Webb, S., 1993. Magma rheology. In: Luth, R.W. (Ed.), Mineralogical Association of Canada Short Course Handbook on Experiments at High Pressure and Applications to the Earth's Mantle 21, pp. 131–196.

Dobran, F., 1992. Nonequilibrium flow in volcanic conduits and application to the eruptions of Mt. St. Helens on May 18, 1980, and Vesuvius in AD 79. J. Volcanol. Geotherm. Res. 49, 285–311.

Druitt, T.H., Sparks, R.S.J., 1984. On the formation of calderas during ignimbrite eruptions. Nature 310, 679–681.

Dudarev, A.N., Kudryavtsev, V.A., Melamed, V.G., Sharapov, V.N., 1972. Heat Transfer in Magmatic Processes. Nauka, Novosibirsk, 124 pp. (in Russian).

Eichelberger, J.C., Carrigan, C.R., Westrich, H.R., Price, R.N., 1986. Nonexplosive silicic volcanism. Nature 323, 598–602.

Epelbaum, M.B., 1980. Silica Melt Containing Volatile Components. Nauka, Moscow, 255 pp. (in Russian).

Escher, B.G., 1933. On the character of the Merapi eruption in central Java. Leidse Geol. Meded. 6, 85–103.

Farberov, A.I., 1979. Magmatic Chambers under Volcanoes of Eastern Kamchatka on the Base of Geophysical Data. Nauka, Novosibirsk, 88 pp. (in Russian).

Fedotov, S.A., 1976a. Geophysical data on magmatic activity in the depth under Kamchatka and estimation of the forces moving magma upward toward volcanoes (in Russian). Izv. AN SSSR Ser. Geol. 4, 5–16.

Fedotov, S.A., 1976b. On the mechanism of the magmatic activity in depth under volcanoes on island arcs and similar structures (in Russian). Izv. AN SSSR Ser. Geol. 5, 25–37.

Fedotov, S.A. (Ed.), 1984. The Great Fissure Tolbachik Eruption, Kamchatka 1975-1976. Nauka, Moscow, 637 pp. (in Russian).

Ferrucci, F., Hirn, A., De Natale, G., Virieux, J., Mirabile, L., 1992. P-SV conversions at a shallow boundary beneath Campi Flegrei caldera (Italy): evidence for the magma chamber. J. Geophys. Res. 97 (B11), 15351–15359.

Giberti, G., Wilson, L., 1990. The influence of geometry on the ascent of magma in open fissures. Bull. Volcanol. 52, 515–521.

Gilmore, R., 1981. Catastrophe Theory for Scientists and Engineers. Wiley–Interscience, New York, 666 pp.

Gorshkov, A.P., 1973. The deep structure of the volcano Maly Semyachik (Kamchatka) by the gravimetrical data (in Russian). Geol. Geofis. 4, 140–142.

Gorshkov, G.S., Bogoyavlenskaya, G.E., 1965. Bezymyanny Volcano and Principal Features of its Last Eruption 1955-1963. Nauka, Moscow, 170 pp. (in Russian).

Graton, L.K., 1945. Conjectures regarding volcanic heat. Am. J. Sci. 243 (A), 135–259.

Gushchenko, I.I., 1979. Volcanic Eruptions of the World (Catalogue). Nauka, Moscow, 475 pp. (in Russian).

Heiken, G., Wohletz, K., 1985. Volcanic Ash. University of California Press, Berkeley, CA, 246 pp.

Hurwitz, S., Navon, O., 1994. Bubble nucleation in rhyolitic melts: experiments at high pressures, temperature and water content. Earth Planet. Sci. Lett. 122, 267–280.

Jaupart, C., Allegre, C., 1991. Gas content, eruption rate and instabilities of eruption in silicic volcanoes. Earth Planet. Sci. Lett. 102, 413–429.

Kadik, A.A., Eggler, D.H., 1976. Water and carbon dioxide regime in the origin and degassing of acid magmas. Geokhimia 2, 163–179.

Kadik, A.A., Lebedev, E.B., Khitarov, N.I., 1971. Water in Magmatic Melts. Nauka, Moscow, 267 pp. (in Russian).

Kadik, A.A., Maximov, A.P., Ivanov, B.V., 1986. Physycochemical Conditions of Crystallization and Genesis of Andesites. Nauka, Moscow, 158 pp. (in Russian).

Kovalev, G.N., 1971. On the energetics of the active volcanism. Volcanism and the Depth of the Earth. Proceedings of the 3rd All-Union Volcanol. Conf. Nauka, Moscow, pp. 41–46 (in Russian).

Kovalev, G.N., Slezin, Yu.B., 1974. Some features of the dynamics of volcanic process. In: Geodynamics, Magma Genesis and Volcanism. Petropavlovsk-Kamchatsky, pp. 287–297 (in Russian).

Kovalev, G.N., Kutyev, F.Sh., 1977. The estimation of the temperature conditions in vigorous ash-gas jets on the Tolbachik eruption 1975 (Kamchatka) by the structure of volcanic bombs (in Russian). Dokl. AN SSSR 237, 1171–1174.

Kovalev, G.N., Slezin, Yu.B., 1979a. The dynamics of magma degassing on the eruption of Southern Breakthrough of the Great fissure Tolbachik eruption 1975-1976 (in Russian). Bull. Volcanol. Stations 56, 15–24.

Kovalev, G.N., Slezin, Yu.B., 1979b. Basaltic scoria structure and composition of the ferriferous minerals (Southern Breakthrough of the Tolbachik eruption 1975-1976) (in Russian). Vulkanol. Seismol. 4, 22–33.

Kovalev, G.N., Kalashnikova, L.V., Slezin, Yu.B., 1971. On the connection between eruptions energy and preceding dormant periods duration of the active volcanoes (in Russian). Geol. Geofis. 3, 137–140.

Kravchenko, V.S., 1955. On the nature and mechanism of coal and gas sudden outbursts (in Russian). Izv. AN SSSR 6, 101–108.

Lacroix, A., 1904. La Montagne Pelèe et ses Eruptions. Masson, Paris, 662 pp.

Lebedev, E.B., Khitarov, N.I., 1979. Physical Properties of Magmatic Melts. Nauka, Moscow, 152 pp. (in Russian).

Letnikov, F.A., 1992. Synergetics of Geological Systems. Nauka, Siberian subdivision, Novosibirsk, 227 pp. (in Russian).

Letnikov, F.A., Kuznetsov, K.E., Medvedev, V.Ya., 1990. On the fluidized silica melts decompression (in Russian). Dokl. AN SSSR 313, 682–685.

Lipman, P.W., 1984. The roots of ash-flow calderas in North America: Windows into the tops of granitic batholiths. J. Geophys. Res. 89, 8801–8841.

Lipman, P.W., 1986. Emplacement of large ash sheets and relation to caldera collapse. In: Int. Volcanol. Congr. Abstracts. New Zealand, p. 58.

Lipman, P.W., Mullineaux, D.R. (Eds.), 1981. The 1980 Eruption of Mount St. Helens, Washington. US Geol. Prof. Paper 1250, 844 pp.

Lister, J.R., 1990. Buoyancy-driven fluid fracture: the effect of material toughness and of low-viscosity precursors. J. Fluid Mech. 210, 263–280.

Luchitsky, I.V., 1971. Foundations of Paleovolcanology, Vol. 1. AN SSSR, Moscow, 480 pp. (in Russian).

Macdonald, G.A., 1963. Physical properties of erupting Hawaiian magmas. Geol. Soc. Am. Bull. 74, 1071–1078.

Murase, T., McBirney, A.R., 1973. Properties of some common igneous rocks and their melts at high temperature. Geol. Soc. Am. Bull. 84, 3563–3592.

McGetchin, T.R., Ullrich, G.W., 1973. Xenoliths in maars and diatremes with inferences for the Moon, Mars and Venus. J. Geophys. Res. 78, 1833–1853.

Melnik, O.E., 2000. Dynamics of two-phase flow of high-viscosity gas-saturated magma: large variations of sustained explosive eruption intensity. Bull. Volcanol. 62, 153–170.

Melnik, O.E., Sparks, R.S.J., 1999. Non-linear dynamics of lava dome extrusion. Nature 402, 37–41.

Menyaylov, I.A., Nikitina, L.P., Shapar, V.N., 1980. Geochemical Features of Exhalations of the Great Fissure Tolbachik Eruption. Nauka, Moscow, 235 pp. (in Russian).

Mercalli, G.I., 1907. Vulcani Attivi della Terra. Milano, 421 pp.

Miller, D.S., Smith, R.B., 1999. P and S velocity structure of the Yellowstone volcanic field from local earthquake and controlled source tomography. J. Geophys. Res. 104, 15105–15121.

Moore, J.G., Lipman, P.W., Swanson, D.A., Alpha, T.R., 1981. Growth of lava domes in the crater, June 1980 - January 1981. In: Lipman, P.W., Mullineaux, D.R. (Eds.), The 1980 Eruption of Mount St. Helens, Washington. US Geol. Prof. Paper 1250, pp. 541–548.

Mysen, B.O., 1977. The solubility of H_20 and CO_2 under predicted magma genesis conditions and some petrological and geophysical considerations. Rev. Geophys. Space Phys. 15, 351–361.

Mysen, B.O., Virgo, D., 1980. The solubility behavior of CO_2 in melts on the join $NaAl_3O_8$-$CaAl_2Si_2O_8$-CO_2 at high pressures and temperatures: a Raman spectroscopic study. Am. Mineral. 65, 1166–1175.

Nigmatullin, R.I., 1987. Multiphase Media Dynamics. Nauka, Moscow. Part I, 370 pp.; Part II, 359 pp. (in Russian).

Papale, P., 1998. Volcanic conduit dynamics. In: Freundt, A., Rosi, M. (Eds.), From Magma to Tephra, Modeling Physical Processes of Explosive Volcanic Eruptions, Developments in Volcanology 4. Elsevier, Amsterdam, pp. 55–89.

Papale, P., Polacci, M., 1999. Role of carbon dioxide in dynamics of magma ascent in explosive eruptions. Bull. Volcanol. 60, 583–594.

Persikov, E.S., 1984. The Viscosity of Magmatic Melts. Nauka, Moscow, 159 pp. (in Russian).

Popov, V.S., 1973. On the mechanics of thin dykes and sills intrusion (in Russian). Izv. AN SSSR Ser. Geol. 10, 48–57.

Poston, T., Stewart, I., 1978. Catastrophe Theory and its Applications. Pitman, London, 510 pp.

Ramberg, H., 1981. Gravity, Deformation and the Earth Crust. Academic Press, London, 425 pp.

Roche, O., Druitt, T.H., Merele, O., 2000. Experimental study of caldera formation (Review). J. Geophys. Res. Solid Earth 105, 395–416.

Rutherford, M.J., Sigurdsson, H., Carey, S., Davis, A., 1985. The May 18, 1980 eruption of Mount St. Helens. 1. Melt composition and experimental phase equilibria. J. Geophys. Res. 90, 2929–2947.

Ryan, M.P., 1987. Neutral buoyancy and the mechanical evolution of magmatic system. In: Mysen, B.O. (Ed.), Magmatic Processes: Physico-chemical Principles. Geochem. Soc. Spec. Publ. no. 1, pp. 259–287.

Sanders, C.O., 1984. Location and configuration of magma bodies beneath Long Valley, California determined from anomalous earthquakes signals. J. Geophys. Res. 89, 8287–8302.

Sarna-Wojcicki, A.M., Shipley, S., Waitt, R.B., Jr., Dzurisin, D., Wood, S.H., 1981. Areal distribution, thickness, mass, volume and grainsize of air-fall ash from the six major eruptions of 1980. In: Lipman, P.W., Mullineaux, D.R. (Eds.), The 1980 Eruption of Mount St. Helens, Washington. US Geol. Prof. Paper 1250, pp. 577–600.

Shanzer, A.E., 1978. Xenoliths of base rocks in the eruption products of the new Tolbachik volcanoes and the problem of magmatic conduits formation in the upper part of the Earth crust. In: Fedotov S.A. (Ed.), Geological and Geophysical Data on the Great Fissure Tolbachik Eruption 1975-1976. Nauka, Moscow, pp. 56–63 (in Russian).

Shaw, H., 1972. Viscosities of magmatic silicate liquids: an empirical method of prediction. Am. J. Sci. 272, 870–893.

Sheymovich, V.S., 1975. Volcanic conduits (in Russian). Geol. geofis. 9, 29–36.

Sheymovich, V.S., Patoka, M.G., 1980. Feeding systems of volcanoes (in Russian). Vulkanol. Seismol. 6, 21–32.

Simkin, T., Siebert, L., 1984. Explosive Eruptions in Space and Time: Durations, Intervals, and a Comparison of the World's Active Belts. Explosive Volcanism: Inception, Evolution and Hazards. National Academy Press, Washington, DC, pp. 110–121.

Simkin, T., Siebert, L., 1994. Volcanoes of the World. Geoscience Press, Tucson, AZ, 349 pp.

Slezin, Yu.B., 1979. The conditions of origin of the dispersion regime in volcanic eruption (in Russian). Vulkanol. Seismol. 3, 69–76.

Slezin, Yu.B., 1980a. Stationary dispersion regime at the explosive volcanic eruptions (in Russian). Vulkanol. Seismol. 2, 56–66.

Slezin, Yu.B., 1980b. Interaction between particles in the stationary gas-pyroclastic flow (in Russian). Vulkanol. Seismol. 5, 40–47.

Slezin, Yu.B., 1982a. The fragmentation level at the stationary dispersion regime of eruption (in Russian). Vulkanol. Seismol. 2, 3–11.

Slezin, Yu.B., 1982b. The dymamics dispersion jet in the explosive volcanic eruption (in Russian). Vulkanol. Seismol. 3, 18–29.

Slezin, Yu.B., 1983. The dynamics of dispersion regime in volcanic eruptions: 1. Theoretical description of magma movement through volcanic conduit (in Russian). Vulkanol. Seismol. 5, 9–17.

Slezin, Yu.B., 1984. The dynamics of dispersion regime in volcanic eruptions: 2. The condition of magma mass rate instability and the nature of catastrophic explosive eruptions (in Russian). Vulkanol. Seismol. 1, 23–35.

Slezin, Yu.B., 1987. Mechanism of magma chamber evacuation leading to caldera formation (in Russian). Vulkanol. Seismol. 5, 3–15.

Slezin, Yu.B., 1990. On some natural features of the strombolian activity on the Southern Breakthrough of Tolbachik eruption 1975-1976 (in Russian). Vulkanol. Seismol. 1, 16–26.

Slezin, Yu.B., 1991. Changes in magma mass rate during a large explosive eruption (in Russian). Vulkanol. Seismol. 1, 35–45.

Slezin, Yu.B., 1994. Dependence of eruption character on magma properties (the results of numerical experiment) (in Russian). Vulkanol. Seismol. 4–5, 121–127.

Slezin, Yu.B., 1995a. Principal regimes of volcanic eruptions. Vulkanol. Seismol. 2, 72–82. (in Russian). English translation in: 1995. Volcanol. Seismol. 17, 193–206.

Slezin, Yu.B., 1995b. Mechanism of extrusive eruptions. Vulkanol. Seismol. 4–5, 76–84. (in Russian). English translation in: 1996. Volcanol. Seismol. 17, 449–460.

Slezin, Yu.B., 1997. Evolution of a volcanic eruption (theoretical treatment) (in Russian). Vulkanol. Seismol. 2, 3–15.

Slezin, Yu.B., 1998. The Mechanism of Volcanic Eruptions (Stationary Model). Nauchny Mir, Moscow, 127 pp.

Slezin, Yu.B., Melnik, O.E., 1994. Dynamics of the volcanic eruption with magma of high viscosity (in Russian). Vulkanol. Seismol. 1, 3–12.

Slobodskoy, R.M., 1977. New type of volcanic bombs (Tolbachik eruption 1975) (in Russian). Dokl. AN SSSR 234, 1429–1532.

Smith, R.L., 1979. Ash-flow magmatism. Geol. Soc. Am. Spec. Paper 180, 5–27.

Smith, R.B., Braile, L.W., 1994. The Yellowstone Hotspot. J. Volcanol. Geotherm. Res. 61, 121–188.

Sparks, R.S.J., 1978. The dynamics of bubble formation and growth: a review and analysis. J. Volcanol. Geotherm. Res. 3, 1–37.

Sparks, R.S.J., Wilson, L., Hulme, G., 1978. Theoretical modelling of the generation, movement and emplacement of pyroclastic flows by column collapse. J. Geophys. Res. 94, 1867–1887.

Sparks, R.S.J., Bursik, M.I., Carey, S.N., Gilbert, J.S., Glaze, L.S., Sifurdsson, H., Woods, A.W., 1997. Volcanic Plumes. Wiley, Chichester, 557 pp.

Sparks, R.S.J., Murphy, M.D., Lejeune, A.M., Watts, R.B., Barclay, J., Young, S.R., 2000. Control on the emplacement of the andesite lava dome of the Soufriere Hills Volcano by degassing-induced crystallization. Terra Nova 12, 14–20.

Spera, F.J., Crisp, J.A., 1981. Eruption volume, periodicity and caldera area: relationships and inferences on development of compositional zonation in silicic magma chambers. J. Volcanol. Geotherm. Res. 11, 169–187.

Stasiuk, M.V., Jaupart, C., Sparks, R.S.J., 1993. On the variations of flow rate in non-explosive lava eruptions. Earth Planet. Sci. Lett. 114, 505–516.

Sternin, L.E., 1974. Foundations of Gas-dynamics of the Flow in Nozzles. Mashinostroenie, Moscow, 212 pp. (in Russian).

Swanson, D.A., Holcomb, R.T., 1990. Regularities in growth of Mount St Helens dacit dome 1980-86. In: Fink, J.H.

(Ed.), Lava Flows and Domes; Emplacement Mechanisms and Hazards Implications. Springer, Berlin, pp. 3–24.

Tokarev, P.I., 1977. Some natural features of a volcanic process. In: Magma Genesis and its Connection with Volcanic Process. Nauka, Moscow, pp. 25–40. (in Russian).

Toramaru, A., 1989. Vesiculation process of ascending magma. J. Geophys. Res. 94, 17523–17542.

Vande-Kirkov, Yu.V., 1978. Viscosity of the lavas of the Northern Breakthrough (Tolbachik), 1975 (in Russian). Bull. Volcanol. Stations 55, 13–17.

Vergniolle, S., Jaupart, C., 1990. Dynamics of degassing of Kilauea volcano, Hawaii. J. Geophys. Res. 95, 2793–2809.

Verhoogen, J., 1951. Mechanics of ash formation. Am. J. Sci. 249, 729–739.

Walker, G.P.I., 1980. The Taupo pumice: product of the most powerful known (ultraplinian) eruption? J. Volcanol. Geotherm. Res. 8, 69–94.

Walker, G.P.I., 1984. Downsag calderas, ring faults, caldera sizes and incremental caldera growth. J. Geophys. Res. 89, 8407–8416.

Walker, G.P.I., Wilson, L., Bowell, F.L.G., 1971. Explosive volcanic eruptions. 1. The rate of fall of pyroclasts. Geophys. J. R. Astron. Soc. 22, 377–383.

Wallis, G., 1969. One-dimension Two-phase Flows. McGraw Hill, New York, 408 pp.

Williams, S.N., Self, S., 1983. The October 1902 plinian eruption of Santa Maria volcano, Guatemala. J. Volcanol. Geotherm. Res. 16, 33–56.

Wilson, L., 1976. Explosive volcanic eruptions III: Plinian eruption columns. Geophys. J. R. Astron. Soc. 45, 543–556.

Wilson, L., Head, J.W., 1981. Ascent and eruption of basaltic magma on the Earth and Moon. J. Geophys. Res. 86, 2971–3001.

Wilson, L., Huang, T.C., 1979. The influence of shape on the atmospheric settling velocity of volcanic ash particles. Earth Planet. Sci. Lett. 44, 311–324.

Wilson, C.J.N., Walker, G.P.L., 1985. The Taupo eruption, New Zealand I. General aspects. Philos. Trans. R. Soc. London A 314, 199–228.

Wilson, L., Sparks, R.S.J., Walker, G.P.J., 1980. Explosive volcanic eruptions - IV. The control of magma properties and conduit geometry on eruption behaviour. Geophys. J. R. Soc. 63, 117–148.

Witham, A.G., Sparks, R.S.J., 1986. Pumice. Bull. Volcanol. 48, 209–223.

Woods, A.W., Koyaguchi, T., 1994. Transitions between explosive and effusive volcanic eruptions. Nature 370, 641–644.

Yokoyama, I., 1969. The subsurfase structure of Oshima volcano Izu. J. Phys. Earth 17, 55–68.

Zlobin, G.I., Fedorchenko, V.I., 1982. Abyssal structure of volcano Golovnina obtained by the analysis of interchange earthquake waves (in Russian). Vulkanol. Seismol. 4, 99–103.

Zubin, M.I., Kozyrev, A.I., 1989. Gravitational model of the volcano Avachinskii structure (Kamchatka) (in Russian). Vulkanol. Seismol. 1, 81–93.

Zubin, M.I., Melekestsev, I.V., Tarakanovsky, A.A., Erlich, E.N., 1971. Quaternary calderas in Kamchatka. Volcanism and the Depth of the Earth. Proceedings of the 3rd All-Union Volcanol. Conf. Nauka, Moscow, pp. 55–66.